

## Successive shifts of the India-Africa transform plate boundary during the Late Cretaceous-Paleogene interval: implications for ophiolite emplacement along transforms

Rodriguez Mathieu <sup>1,\*</sup>, Huchon Philippe <sup>2</sup>, Chamot-Rooke Nicolas <sup>1</sup>, Fournier Marc <sup>2</sup>, Delescluse Matthias <sup>1</sup>, Smit Jeroen <sup>3</sup>, Plunder Alexis <sup>2</sup>, Calvès G r me <sup>4</sup>, Ninkabou Dia <sup>1,2</sup>, Pubellier Manuel <sup>1</sup>, Fran ois Thomas <sup>5</sup>, Agard Philippe <sup>2</sup>, Gorini Christian <sup>2</sup>

<sup>1</sup> Laboratoire de G ologie, Ecole normale sup rieure, PSL research university, CNRS UMR 8538, 24 rue Lhomond, 75005 Paris, France

<sup>2</sup> Sorbonne Universit , CNRS-INSU, Institut des Sciences de la Terre de Paris, IStEP UMR 7193, F-75005 Paris, France

<sup>3</sup> Department of Earth Sciences, Utrecht University, PO box 80.021, 3508 TA, Utrecht, The Netherlands

<sup>4</sup> Universit  Toulouse 3, Paul Sabatier, OMP-GET, 14 Avenue Edouard Belin, 31400-F, Toulouse, France

<sup>5</sup> GEOPS, Univ. Paris-Sud, CNRS, Universit  Paris-Saclay, 91405 Orsay, France

\* Corresponding author : Mathieu Rodriguez, email address : [rodriguez@geologie.ens.fr](mailto:rodriguez@geologie.ens.fr)

### Abstract :

The Arabian Sea in the NW Indian Ocean is a place where two major transform boundaries are currently active : the Owen Fracture Zone between India and Arabia and the Owen Transform between India and Somalia. These transform systems result from the fragmentation of the India-Africa Transform boundary, which initiated about 90 Myrs ago, when the India-Seychelles block separated from Madagascar to move towards Eurasia. Therefore, the geological record of the Arabian Sea makes it possible to investigate the sensitivity of a transform system to several major geodynamic changes.

Here we focus on the evolution of the India-Africa transform system during the ~47-90 Ma interval. We identify the Late Cretaceous (~90-65 Ma) transform plate boundary along Chain Ridge, in the North Somali Basin. From 65 to ~42-47 Ma, the India-Africa transform is identified at the Chain Fracture Zone, which crossed both the Owen Basin and the North East Oman margin. Finally, the transform system jumped to its present-day location in the vicinity of the Owen Ridge. These shifts of the India-Africa boundary with time provide a consistent paleogeographic framework for the emplacement of the Masirah Ophiolitic Belt, which constitutes a case of ophiolite emplaced along a transform boundary. The successive locations of the India-Africa boundary further highlight the origin of the Owen Basin lithosphere incoming into the Makran subduction zone.

---

## Highlights

► The Late Cretaceous India-Africa Transform plate boundary is identified at Chain Ridge. ► The Paleogene India-Africa transform plate boundary is identified at the Chain Fracture Zone and within the Owen Basin. ► The Masirah ophiolites emplaced along a transform boundary. ► The oceanic lithosphere subducting nowadays beneath Makran derives from the East Somali Basin instead of Neotethys.

**Keywords** : Transform boundaries, Arabian Sea, Masirah ophiolites

39 **1. Introduction**

40 Transform plate boundaries experience episodes of structural reorganization and migration related to  
41 geodynamic changes (e.g., the San Andreas and Queen Charlotte Faults: DeMets and Merkouriev,  
42 2016; the Levant Fault: Smit *et al.*, 2010; the North Anatolian Fault: Hubert-Ferrari *et al.*, 2009;  
43 LePichon *et al.*, 2016; the Saint Paul transform: Maia *et al.*, 2016). In the oceanic domain, several  
44 transform systems have been active over more than 100 Myrs (Bonatti and Crane, 1982; Ligi *et al.*,  
45 2002; Maia *et al.*, 2016; Maia, 2018), which allows us to investigate their behavior in the wake of  
46 major geodynamic changes.

47 Transform motion between India and Africa started around 90 Ma, when rifting began between  
48 Madagascar and the India-Seychelles block (Bernard and Munsch, 2000; Shuhail *et al.*, 2018). Since  
49 then, Africa has been split into different plates, including Arabia and Somalia, which still have active  
50 transform boundaries with India at the Owen Fracture Zone and the Owen transform, respectively  
51 (Fig. 1; Fournier *et al.*, 2008a, b; 2011; Rodriguez *et al.*, 2011). The India-Africa transform plate  
52 boundary therefore constitutes a good case-study to investigate the response of an oceanic transform  
53 system to geodynamic changes on the 100-Myr scale. The sensitivity of the India-Africa transform  
54 system since the Late Paleogene (~24 Ma) is described in Rodriguez *et al.* (2011; 2013; 2014a,b;  
55 2016; 2018). However, the geological description of this transform fault is largely incomplete for the  
56 Late Cretaceous-Paleogene, a period marked by two major global plate reorganization events at 63-73  
57 Ma (Cande and Patriat, 2015) and 42-47 Ma (Matthews *et al.*, 2016).

58 The aim of the present study is to identify the successive locations and configurations of the India-  
59 Africa transform boundary during this time interval, based on geological and free-air gravity maps, as  
60 well as seismic profiles crossing the Owen and the North Somali Basins. The successive shifts of the  
61 India-Africa transform boundary shed light onto 1) the mode of emplacement of the Masirah  
62 Ophiolite, and of the Bela, Muslim Bagh, Zhob, and Waziristan-Khost ophiolites in Pakistan and  
63 Afghanistan (Fig. 1), and on 2) the origin of the oceanic lithosphere presently subducting under  
64 eastern Makran (Pakistan).

65

66 **2- Geological background & paleogeographic constraints**

## 67 ***2-1- Opening of the Indian Ocean***

68 From the Jurassic to the Cenomanian, two subduction zones drove the fragmentation of  
69 Gondwanaland and the subsequent opening of the Indian Ocean (Norton and Selater, 1979; Besse and  
70 Courtillot, 1988; Seton *et al.*, 2012; Matthews *et al.*, 2012): the Northern Neotethys Subduction  
71 (nowadays recorded along the Indus-Yarlong-Tsangpo suture zone) and the East Gondwana  
72 Subduction (which was located to the East of Australia and Antarctica Plates). A global plate  
73 reorganization event at 100-105 Ma corresponds to the initiation of a new subduction in the Southern  
74 Neotethys Ocean, while the East Gondwana subduction deactivated (Matthews *et al.*, 2012; Jolivet *et*  
75 *al.*, 2016). A late consequence of the 100-105 Ma plate reorganization event is the onset of the  
76 northwards migration of India in the Late Cretaceous (84-87 Ma; Fig. 2; Bernard and Munsch, 2000;  
77 Calvès *et al.*, 2011; Matthews *et al.*, 2012; Gibbons *et al.*, 2013; Battacharya and Yateesh, 2015).  
78 India's northwards drift is disturbed in the Late Maastrichtian, resulting in major changes in  
79 configuration of Indian Ocean's spreading centers. This change is recorded by the bending of fracture  
80 zones since chron 33 (74 Ma) at the SW Indian Ridge (Cande and Patriat, 2015) and a series of ridge  
81 jumps from the Mascarenes spreading centers to the Gop basin and eventually, the Carlsberg Ridge  
82 since 63 Ma (Royer *et al.*, 2002).

83 Seafloor spreading rates at the Carlsberg Ridge peaked at  $18 \text{ cm.yr}^{-1}$  at 52 Ma, before slowing down  
84 due to the onset of a global plate reorganization event, partly related to collision between India and the  
85 Kohistan-Ladakh arc (Burg, 2011; Cande and Stegman, 2011; Bouilhol *et al.*, 2013; Jagoutz *et al.*,  
86 2015; Cande and Patriat, 2015). However, the role of India-Eurasia collision over global plate  
87 dynamics is still highly debated due to uncertainties in its precise timing (see the various  
88 paleogeographic scenarios proposing ages of collision between 24 and 55 Ma in Patriat and Achache,  
89 1984; Chaubey *et al.*, 2002; Ali *et al.*, 2008; Molnar and Stock, 2009; van Hinsbergen *et al.*, 2012;  
90 Gibbons *et al.*, 2015; Matthews *et al.*, 2015; Buckman *et al.*, 2018). Regardless of the precise timing  
91 of the India-Eurasia collision, the Indian Ocean's fabric documents a global plate reorganization event  
92 between 47 and 42 Ma, expressed by changes in spreading rates and trends, as well as a major ridge  
93 jump from the Wharton Basin to the South East Indian Ridge (Coffin *et al.*, 2002).

95 **2-2. The fragmentation of the India-Seychelles-Madagascar block**

96 The series of global plate reorganization events that shaped the Indian Ocean induced several episodes  
97 of breakup within the India-Madagascar block initially separated from Africa and Australia in the Late  
98 Jurassic (Gibbons *et al.*, 2013).

99 First, a mid-oceanic ridge active during Albian-Senonian isolated the Kabul Block continental sliver  
100 from India (Fig. 2; Tapponnier *et al.*, 1981; Gnos and Perrin, 1997; Gaina *et al.*, 2015).

101 Second, a Late Cretaceous break-up between Madagascar and the India-Laxmi-Seychelles continental  
102 blocks (Fig. 1) led to the opening of the Mascarene and the East Somali Basins (Fig. 2; Schlich, 1982;  
103 Bernard and Munsch, 2000; Calvès *et al.*, 2011; Gibbons *et al.*, 2013; Gibbons *et al.*, 2015;  
104 Battacharya and Yateesh, 2015; Shuhail *et al.*, 2018).

105 Third, the break-up between the Seychelles-Laxmi block and India formed the Gop Basin (between  
106 magnetic chrons 31 (68 Ma) and 30 (67 Ma; Minshull *et al.*, 2008; Yateesh *et al.*, 2009; Eagles and  
107 Hoang, 2014). Following the culmination of the Deccan trap volcanism at ~65.5 Ma (Courtilot and  
108 Renne, 2003; Hooper *et al.*, 2010), the onset of the Carlsberg Ridge at chron 28 (63 Ma) marks the full  
109 Laxmi-Seychelles break-up (Dyment, 1998; Royer *et al.*, 2002).

110

111 **2-3- Late Cretaceous-Early Paleocene ophiolites in the NW Indian Ocean**

112 Ophiolites are remnants of oceanic lithosphere emplaced over continental lithosphere that are mainly  
113 encountered in fossil convergence zones, but also in contexts such as transform boundaries (Dilek and  
114 Furnes, 2014). To avoid any confusion, we use the term of ‘*obduction*’ where the ophiolites can be  
115 related to a subduction zone, and the term of ‘*ophiolite emplacement*’ where the ophiolite cannot be  
116 unambiguously tied to a subduction zone.

117 The initiation of an intra-oceanic subduction ~100-105 Ma in the southern part of the Neotethys  
118 Ocean led to obduction north of Arabia and India during the Campanian (Hacker *et al.*, 1996; Agard *et al.*,  
119 2007, 2011; Hébert *et al.*, 2012; Morris *et al.*, 2017; Nicolas and Boudier, 2017; Guilmette *et al.*,  
120 2018). In the surroundings of the Arabian Sea, the related ophiolites are the Semail in Oman (Searle  
121 and Cox, 1999; Breton *et al.*, 2004) and Zhob-Waziristan-Khost ophiolites in NE Pakistan  
122 (Cassaigneau, 1979; Badshah *et al.*, 2000; Sarwar, 1992; Khan *et al.*, 2007).

123 In south east Pakistan, the Bela and Muslim Bagh ophiolites record a different timing of subduction  
124 initiation, ranging between 65-70 Ma from the dating of metamorphic soles (Allemann, 1979;  
125 Mahmood *et al.*, 1995; Gnos *et al.*, 1998; Khan *et al.*, 2007), and 80 Ma from dating of Supra-  
126 Subduction Zone lavas (Kakar *et al.*, 2014). These ophiolites are derived from the basin extending  
127 between India and the Kabul Block.

128 The Masirah Ophiolite running along eastern Oman (Fig. 1) has a different paleogeographic origin.  
129 The oceanic crust exposed in the Masirah Ophiolite was formed at a latitude of ~30-50°S (Gnos and  
130 Perrin, 1997) in Tithonian-Berriasian times (~140-145 Ma; Peters and Mercolli, 1998). These  
131 ophiolites are therefore remnants of the Indian Ocean formed during the early stages of Gondwanaland  
132 break-up. The oldest Arabia-derived sediments (detrital Fayah formation) date back to Coniacian at  
133 Masirah (Immenhauser, 1996), indicating that the Masirah ophiolite was a part of India's lithosphere  
134 prior to its obduction (Gnos *et al.*, 1997). A particularity of the Masirah Ophiolite is the lack of  
135 metamorphic sole and hence, possibly no relationship to subduction (Wakabayashi and Dilek, 2003;  
136 Agard *et al.*, 2016). The age of emplacement is defined from stratigraphic and structural constraints  
137 (Immenhauser, 1996; Schreurs and Immenhauser, 1999; Immenhauser *et al.*, 2000). Late  
138 Maastrichtian folds affecting deep-sea sediments in the Batain plain record the first step of  
139 emplacement, whereas unconformable, Priabonian shallow water carbonates seal the ophiolite.

140

#### 141 ***2-4- The Oman abyssal plain and the Owen Basin***

142 The oceanic lithosphere incoming into the present-day Makran Subduction Zone is 70 to 100 Myrs-old  
143 according to heat flow measurements (Hutchison *et al.*, 1981), similar to ophiolites exposed at Semail.  
144 As a result, the lithosphere of the Oman abyssal plain is generally considered as a remnant of the  
145 Neotethys Ocean (McCall, 1997; Ravaut *et al.*, 1997; 1998; Ellouz-Zimmerman *et al.*, 2007; Barrier  
146 and Vrielynck, 2008; Frizon de Lamotte *et al.*, 2011; Burg, 2018).

147 However, offshore eastern Oman, most of the Owen basin basement is of Paleogene age (Fig. 3;  
148 Mountain and Prell, 1990; Rodriguez *et al.*, 2016). Considering a Neotethys origin for the entire Oman  
149 abyssal plain would imply that the Indian Ocean Tithonian lithosphere facing Arabia during the Late  
150 Maastrichtian emplacement of the Masirah ophiolites (Peters and Mercolli, 1998) must have been

151 subducted between the Owen Basin and the Oman abyssal plain. Such a subduction zone is not  
152 documented, however, questioning the fate of the Tithonian lithosphere now represented by the  
153 Masirah ophiolite, and the origin of the Late Cretaceous lithosphere in the eastern part of the Oman  
154 abyssal plain (Rodriguez *et al.*, 2016).

155 In addition, several features of the Oman abyssal plain remain enigmatic, including the Sonne  
156 lineament and the Qalhat Seamount-Little Murray Ridge (Fig. 3). Although the NW-SE trending  
157 Sonne lineament imaged on the free-air gravity map (Fig. 3) has been first interpreted as a still active  
158 strike-slip fault (Kukowski *et al.*, 2001), no trace of activity has been observed on seismic lines  
159 acquired since (Mouchot, 2009). The Qalhat Seamount and Little Murray Ridge constitute a chain of  
160 submarine volcanoes of Late Cretaceous age (Edwards *et al.*, 2000; Mouchot, 2009) whose  
161 paleogeographic origin remains unclear.

162

### 163 **3- Materials and Methods**

#### 164 ***3-1- Geological, free-air gravity maps and plate reconstructions***

165 The free-air gravity maps (Figs. 3, 4) have been designed using the DTU 13 database filtered for short  
166 wavelengths (Andersen *et al.*, 2013). Offshore, a few multibeam tracks have been acquired in the area  
167 of the Chain Ridge (Fig. 5) during transits of the AOC and VARUNA-CARLMAG cruises onboard  
168 the BHO Beautemps-Beaupré operated by the French navy in 2006 and 2019. The structure of the  
169 strike-slip fault system crossing the Huqf desert in Oman (Fig. 6) is mapped after geological maps of  
170 Oman at 1: 250 000 (sheets of Duqm, Madreka, Khalouf by Platel *et al.*, 1992) and maps built from  
171 seismic data (Filbrandt *et al.*, 2006). The paleogeographic reconstructions of India and Africa  
172 continents are drawn after the Gplates files provided in Matthews *et al.* (2016). The successive  
173 locations of the India-Africa plate boundary identified hereafter complete these reconstructions.

174

#### 175 ***3-2- Seismic reflection***

##### 176 ***3-2-1. Sources of the datasets***

177 For the Owen Basin, we use the seismic dataset from the OWEN 2 survey (Figs. 7 to 10; Rodriguez *et*  
178 *al.*, 2016), acquired in 2012 onboard the R/V Beautemps-Beaupré using a high-speed (10 knots)

179 seismic device. The source consists in two GI air-guns (one 105/105 c.i. and one 45/45 c.i.) fired every  
180 10 seconds at 160 bars in harmonic mode, resulting in frequencies ranging from 15 to 120 Hz. The  
181 receiver is a 24-channel, 300-m-long seismic streamer, allowing a common mid-point spacing of 6.25  
182 m and a sub-surface penetration of about 2 s two-way travel time. The standard processing consisted  
183 of geometry setting, water-velocity normal move-out, stacking, water-velocity f-k domain post-stack  
184 time migration, bandpass filtering and automatic gain control.

185 New interpretations for seismic lines crossing the North Somali Basin (Fig. 4) and the Batain plain in  
186 NE Oman (Fig. 11) are based on the dataset published in Bunce and Molnar (1977) and Beauchamp et  
187 al. (1995), respectively.

188

### 189 *3-2-2. Stratigraphy in the Owen Basin*

190 Seismic profiles have been tied to drilling sites available in the Arabian Sea from DSDP and ODP legs  
191 (Shipboard Scientific Party, 1974a, 1974b, 1989) and stratigraphic details can be found in Rodriguez  
192 *et al.* (2016). Two key seismic horizons have been identified on the seismic lines (Figs. 7 to 10). The  
193 cross-section of the Oman margin provided in Figure 7 summarizes the stratigraphic framework of the  
194 area. A first key reflector corresponds to an angular unconformity recording the end of the uplift of  
195 marginal ridges along the Oman margin in the Late Eocene. This unconformity is only recognized in  
196 the western part of the Owen Basin, and becomes concordant to the east. A second Late Oligocene-  
197 Early Miocene unconformity is observed across the entire Owen Basin, and reflects the diachronous  
198 flooding of the Owen Basin by the Indus turbiditic system (Rodriguez *et al.*, 2016). Finally, the top of  
199 the Masirah Ophiolites, expressed by a chaotic and highly reflective body on seismic lines (Fig. 7, 11),  
200 is considered as Late Maastrichtian, in agreement with onland studies (Immenhauser *et al.*, 1996;  
201 Immenhauser *et al.*, 2000).

202

## 203 **4- Configurations of the India-Africa plate boundary during the Late Cretaceous-** 204 **Eocene**

### 205 *4-1- Configuration of the Late Cretaceous India-Africa plate boundary*



206 In the northern Somali Basin, on the western edge of the NE-SW trending Chain Ridge, a large sub-  
207 vertical fault (offset over  $\sim 2$  s TWT) is imaged on the seismic profile (Fig. 4; Bunce and Molnar,  
208 1977). The fault lineament is well-expressed on the free-air gravity field, and partly mapped on the  
209 multibeam coverage of Chain Ridge (Fig. 5). This fault juxtaposes two different oceanic lithospheres.  
210 On the eastern flank of Chain Ridge, gabbros dredged at DSDP Site 235 indicate a 90 Myrs-old  
211 seafloor (Shipboard Scientific Party, 1974a), i.e., a piece of the East Somali Basin. For the seafloor  
212 west of Chain Ridge, magnetic anomalies document a Late Jurassic to Early Cretaceous age (160 to  
213 130 Ma; Cochran, 1988; Gaina *et al.*, 2015). The western part of the northern Somali Basin is  
214 therefore a remnant of the first stage of opening of the Indian Ocean. The juxtaposition of oceanic  
215 lithospheres of different ages is explained by considering the fault observed west of Chain Ridge as  
216 the fossil Late Cretaceous India-Africa transform plate boundary (Chain Ridge Transform, Fig. 4).

217 Evidence for Late Cretaceous (Santonian-Campanian) left-lateral strike-slip tectonics is further  
218 identified in Oman (Fig. 6). Three-dimensional seismic reflection data document a distributed system  
219 of conjugate strike-slip faults, which display typical flower structures, previously mapped by Filbrandt  
220 *et al.* (2006). Left-lateral faults are also widely observed in the Huqf desert (Oman), cutting through  
221 outcrops of Neoproterozoic remnants of the Pan-African orogeny, at the Khufai, Buah, Shuram,  
222 Mukhaibah and Haushi anticlines (Fig. 6; Shackleton and Ries, 1990; Allen, 2007). This set of  
223 observations defines the NW-SE trending transtensive Haushi-Nafun-Maradi Fault System (HNMFS  
224 hereafter), mapped in Figs. 3 and 6. The HNMFS was active only during the deposition of the Fiqq  
225 formation in Early Maastrichtian (Filbrandt *et al.*, 2006) and also locally accompanied by volcanic  
226 activity (Glennie *et al.*, 1974; Wyns *et al.*, 1992).

227 Despite a poor sedimentary record due to low sedimentation rates during Late Maastrichtian-Early  
228 Paleogene, the seismic lines crossing the western part of the Owen Basin at various latitudes document  
229 some sedimentary layers beneath the Late Maastrichtian horizon sealing the Masirah ophiolites (Figs.  
230 8-10). These Late Maastrichtian-Early Paleocene layers are trapped in half-graben structures and  
231 display a fanning configuration (Figs. 8-10), which reflects tectonic activity. The low density of  
232 available seismic lines does not allow us to map accurately these grabens and their precise relationship

233 with the HNMFS, but they are likely coeval with the tectonic deformation observed along the  
234 HNMFS.

235

#### 236 ***4-2- Configuration of the Paleocene-Eocene India-Africa plate boundary***

237 In the North Somali Basin, the Paleocene-Eocene India Africa plate boundary is expressed as the  
238 Chain Fracture Zone (Figs. 1, 4), which bounds the seafloor accreted at the Carlsberg Ridge since 63  
239 Ma (Royer et al., 2002; Chaubey et al., 2002). However, the trace of the India-Africa transform  
240 boundary has not been clearly identified offshore Arabia in the Owen Basin, due to the complex  
241 history of the area related to various episodes of margin reactivation (*Rodriguez et al.*, 2014, 2016). In  
242 this section we explore the remnants of the Paleocene-Eocene India Africa plate boundary preserved  
243 along the East Oman Margin and the Owen Basin.

#### 244 *Eastern Oman margin -Masirah :*

245 The free-air gravity map of the Oman margin (Fig. 3) documents a series of en-échelon marginal  
246 ridges within a ~90-km-wide, N30°E-trending corridor running from Sawqirah to Ras Al Hadd (over  
247 ~600 km). The seismic line displayed in Fig. 11 (from *Beauchamp et al.*, 1995) crosses the Masirah  
248 Ophiolite onshore, in one of the few places where the initial structure of the ophiolite is still preserved.  
249 There, the Masirah Ophiolites display a double vergent thrust stack of numerous ophiolite sheets,  
250 according to our revised interpretation (Fig. 11; *Beauchamp et al.*, 1995). The cross section and the  
251 profiles displayed in Fig 7 show that elsewhere along the en-échelon marginal ridge system, the  
252 offshore segments of the Masirah Ophiolites are scattered. Vertical fault offsets (Fig. 7) indicate that  
253 the initial Masirah Ophiolite has been highly dismembered during the formation (i.e., uplift and  
254 shearing) of the en-échelon marginal ridge system (Fig. 3).

255 The stratigraphy of the eastern Oman margin documents the period of formation of this system of en-  
256 échelon marginal ridges. Onland, the Masirah ophiolite overlies a Late Maastrichtian, deep-sea detrital  
257 formation (Fayah Fm; *Immenhauser*, 1996), indicating that the marginal ridges did not exist at that  
258 time. On the other hand, the Priabonian shallow-water carbonates of the Aydim formation and laterites

259 cover both the ophiolites and the marginal ridges (Immenhauser, 1996; Shipboard Scientific Party,  
260 1989). The Aydim formation is coeval with a major angular unconformity along the edges of the  
261 marginal ridges in the Owen Basin, marking the end of the marginal ridge uplift (Figure 3, 7;  
262 Rodriguez *et al.*, 2016). The uplift of the en-échelon system of marginal ridges therefore lasted over  
263 more than 25 Myrs, from 65-70 Ma up to ~40 Ma. This period is coeval with numerous geological  
264 events identified along the east Oman margin, including alkaline volcanism in the Batain and Haushi-  
265 Huqf areas (Gnos and Peters, 2003), and a reorganization of detrital sedimentary systems in SE Oman  
266 consistent with surface uplift (Filbrandt *et al.*, 2006; Robinet *et al.*, 2013).

#### 267 *Owen Basin:*

268 The seismic lines displayed in Figs. 8 to 10 document the structural expression of the Paleogene India-  
269 Africa plate boundary within the Owen Basin, at various latitudes. In all these lines, we map the area  
270 where the indicators of pre-Late Maastrichtian tectonics vanish within the Owen Basin (Figs. 8-10).  
271 The area bounding the Late Maastrichtian basins displays a V-shape typical of transform valleys, with  
272 flanks characterized by a ~30° slope, shaped by erosion due to bottom current and mass wasting  
273 (frequently observed on figs. 8-10). Due to the low sedimentation rates during the Paleogene, the  
274 preservation of this extinct transform structure in the geological record is poor.

275 The location of the Chain Fracture Zone according to reconstructions by Royer *et al.* (2002) coincides  
276 with the eastern boundary of the pre-Maastrichtian basins identified on the seismic lines (Figs. 8-10).  
277 In reconstructions, the Chain Fracture Zone follows the trend of the northeast Oman margin north of  
278 20°N (Fig. 3), where its steepness is compatible with a transform margin. The eastern part of the Owen  
279 Basin is Paleogene in age, consistent with basement ages obtained at ODP drilling sites along the  
280 Owen Ridge (Shipboard Scientific Party, 1974b, 1989). The composite age of the basement may  
281 therefore be explained by a major transform boundary crossing the Owen Basin (Fig. 3, Rodriguez *et*  
282 *al.*, 2016).

283

## 284 **5- Discussion**

285 Identification or reappraisal of these structural relationships highlight a major change in the  
286 configuration of the India-Africa boundary around ~65-70 Ma (i.e., coeval with the global plate  
287 reorganization event; Cande and Patriat, 2015). Data indicate that the India-Africa plate boundary  
288 migrated from the Chain Ridge Transform to the Chain Fracture Zone (Fig. 12). Here we address  
289 critical points of the structural evolution of the India-Africa plate boundary raised by the  
290 reconstruction of figure 12, as well as the paleogeographic implications of the transform plate  
291 boundary migration.

### 292 *5-1-Structural evolution of the India-Africa plate boundary during the Late Cretaceous-Eocene*

293 For the Late Cretaceous India-Africa plate boundary, our reconstruction highlights a lack of direct  
294 connection between the Chain Ridge transform offshore Somalia and the HNMFS in Oman (Fig. 12).  
295 While the HNMFS could be a distributed strike-slip system related to the partitioning of India-Africa  
296 motion along the offshore Chain Ridge Transform ( Filbrandt *et al.*, 2006), its trend may reflect older  
297 Neoproterozoic structures (Allen, 2007) reactivated in response to the complex Late Cretaceous stress  
298 field, influenced by both the obduction of the Semail to the north and transform tectonics to the east.

299 For the Paleocene-Middle Eocene India-Africa plate boundary, the development of the en-échelon  
300 system of marginal ridges constitutes the clearest record of transform fault activity. The en-échelon  
301 system of marginal ridges may be interpreted as the result of a sheared transform margin (Fig. 13), in a  
302 transpressive, partitioned left-lateral strike-slip system of deformation related to the Chain Fracture  
303 Zone between ~65-70 Ma and ~40-45 Ma. Strain partitioning may explain the development of the  
304 marginal ridges along the southern part of the Oman margin, which was located more than 100 km  
305 away from the Chain Fracture Zone. In this framework, the en-échelon system of marginal ridges  
306 results from the reactivation of Tithonian passive margin structures, and probably structures  
307 reactivated during the activity of the HNMFS (Fig. 13; see below).

308 Trehu *et al.* (2015) demonstrated for a similar marginal ridge at the Queen Charlotte Transform  
309 (Carlson *et al.*, 1988; Barrie *et al.*, 2013; Rhor 2015) that such a configuration is typical of a slight  
310 (<15°) component of oblique convergence inducing transpression.

311

### 312 ***5-2- Emplacement of the Masirah Ophiolite along the east Oman transform margin***

313 These results allow to reappraise the emplacement of the Masirah ophiolite of Jurassic age (Fig. 13).  
314 The story begins during the Late Maastrichtian, coeval with the migration of the India-Africa plate  
315 boundary at ~65-70 Ma from Chain Ridge to the Chain Fracture Zone. Paleogeographic  
316 reconstructions show that the Chain Fracture Zone must have crossed the Owen basin and the  
317 northeastern Oman margin in the area of the Batain plain (Royer *et al.*, 2002; Fournier *et al.*, 2010;  
318 Rodriguez *et al.*, 2016). There, the Masirah Ophiolite was a double vergent structure (Fig. 11) formed  
319 along a transpressive segment of the Chain Fracture Zone, or a remnant of Chain Ridge passing by the  
320 Chain Fracture Zone. The Masirah Ophiolite is uplifted during the Paleogene, when the en-échelon  
321 marginal ridges of the Oman transform margin developed (Fig. 10). During the Paleocene-Eocene,  
322 distributed left-lateral shear and uplift of the marginal ridges promoted the dismembering of the  
323 ophiolite fragments initially located in the Batain plain (Fig. 13). Dismembering of the ophiolites  
324 within the shear zone would explain why the double vergent structure identified at the Batain, as well  
325 as the fold system in front of the ophiolites (Schreurs and Immenhauser, 1999), are no longer observed  
326 to the south at Sawqirah or Masirah.

327 The initial double-vergent structure proposed for the Masirah ophiolites along the Chain Fracture Zone  
328 is very similar to many transverse ridges observed worldwide, such as the Davie Ridge offshore  
329 Mozambique (Mahanjane, 2014), the St Paul transverse ridge in the Atlantic (Maia *et al.*, 2016) or the  
330 MacQuarie Ridge at the Australia-Pacific plate boundary (Meckel *et al.*, 2003). The fact that double  
331 vergent structures may be a favorable setting for the initiation of ophiolite emplacement has already  
332 been proposed for the Meratus ophiolite in SE Borneo (Pubellier *et al.*, 1999) along an oblique  
333 convergent plate boundary.

### 334 ***5-3-Paleogeographic implications***

335 Figure 14 presents paleogeographic reconstructions, which emphasize the successive locations of the  
336 India-Africa boundary and the related transfer of fragments of oceanic lithosphere from one plate to  
337 another. The migration of the India-Africa plate boundary from the Chain Ridge to the Chain Fracture  
338 Zone around 65-70 Ma induced a transfer of a sliver of Late Cretaceous oceanic lithosphere from the

339 East Somali Basin to Africa, explaining the age contrast with the western part of the North Somali  
340 Basin (Fig. 14c). The Late Cretaceous lithosphere from the East Somali Basin was displaced  
341 northwards along the Chain Fracture Zone, while seafloor was formed at Carlsberg Ridge (Fig. 14d).  
342 The plate boundary then jumped to its present-day location along the Owen Ridge, during the Late  
343 Eocene-Oligocene (Rodriguez *et al.*, 2016), probably as a consequence of India-Eurasia collision and  
344 the global plate reorganization event recorded around 47 Ma (Müller *et al.*, 2016). This migration of  
345 the India-Africa plate boundary lead to another episode of transfer to Africa of a piece of the oceanic  
346 lithosphere accreted at the Carlsberg Ridge (Fig. 14e; Rodriguez *et al.*, 2016). In this reconstruction,  
347 the composite origin of the Owen Basin is explained by the juxtaposition of remnants of a Tithonian  
348 passive margin to the west, slices of a Tithonian proto-Indian Ocean lithosphere preserved along the  
349 Masirah ophiolite, and Paleogene lithosphere formed at the Carlsberg Ridge to the east (Fig. 14).  
350 Therefore, the Late Cretaceous lithosphere subducting in front of the Makran has two different  
351 paleogeographic origins (Fig. 14): the Neotethys west of the Chain Fracture Zone and the East Somali  
352 Basin to the east (east of  $\sim 61^\circ\text{E}$ ).

353 This scenario also provides an explanation for the paleogeography of the Tithonian lithosphere at the  
354 origin of the Masirah ophiolite, that does not require a subduction zone between the Owen Basin and  
355 the Oman abyssal plain (Fig. 14). The East Somali Basin spreading center formed within the Tithonian  
356 oceanic lithosphere at the origin of the ophiolites, or at the tip of the Lower Cretaceous basin located  
357 between India and the Kabul block (Fig. 14). During the Late Cretaceous, the Tithonian lithosphere  
358 was progressively displaced to the north along the Chain Ridge Transform, while the East Somali and  
359 Mascarenes Basins opened to the south (the spreading center being at the tip of the Chain Ridge  
360 Transform). In the Late Maastrichtian, when the Masirah ophiolite emplacement started (unrelated to  
361 any subduction), the Tithonian lithosphere had reached the latitude of Oman (Fig. 12,14). After the  
362 Masirah obduction, the remaining Tithonian lithosphere located east of the Chain Fracture Zone was  
363 subducted beneath eastern Makran (Figs. 14c,d). In detail, this reconstruction suggests that the Sonne  
364 lineament, Qalhat seamount and Little Murray Ridge (Fig. 3) are parts of the fossil ocean-ocean  
365 transition between the East Somali Basin and the Carlsberg seafloor, when the Carlsberg Ridge  
366 formed in the wake of the Deccan plume (Dyment, 1998).

367 With regards to the eastern Pakistan ophiolites, the India-Africa plate boundary was located west of  
368 the Kabul block in the Late Maastrichtian according to our reconstruction (Fig. 14), making it difficult  
369 to consider these ophiolite sequences as remnants of an India-Africa transform, unless a complex  
370 stepover is involved. Instead, during the Paleogene-Early Eocene, the trend of the Chain Fracture Zone  
371 allows a connection with the Sistan Ocean (Fig. 14; Treolar and Izatt, 1993; McCall, 1997). More  
372 constraints from the surroundings of the Kabul block are needed to further document this episode of  
373 transform tectonics.

374

375 ***5-4- Migration of the India-Africa plate boundary at ~74-63 Ma as part of a global plate***  
376 ***reorganization event?***

377 The reorganization of the India-Africa plate boundary identified around 74-63 Ma may result from a  
378 major geodynamic reorganization event affecting the entire Indian Ocean. The driver of this plate  
379 reorganization event is a matter of debate. The Indonesian Slab reached the Lower Mantle during this  
380 period, which affects the slab pull force (Faccenna *et al.*, 2013). The volcanic activity of the Deccan-  
381 Réunion Plume peaked at 65 Ma, but earliest traces of Deccan type volcanism are encountered around  
382 110-120 Ma (Mahoney *et al.*, 2002). Both slab penetration into the lower mantle and plume-push may  
383 affect oceanic spreading patterns at mid-oceanic ridges and global plate dynamics (Cande *et al.*, 2011;  
384 van Hinsbergen *et al.*, 2011; Faccenna *et al.*, 2013), even if the relative contribution of each process to  
385 force balance remains a matter of debate (Anderson, 2001; Bercovici, 2003; Cande and Stegman,  
386 2011). However, these processes do not explain the abrupt change in plate boundary configuration.

387 Two punctual geological events (duration <5 myrs) may have contributed to the plate boundary  
388 reorganization event by affecting subduction dynamics (boundary forces):

389 - deactivation of the subduction at the origin of the Bela and Muslim-Bagh ophiolites and the Masirah  
390 Slab in tomography (Gaina *et al.*, 2015);

391 - collision of the Woyla Arc (Wajzer *et al.*, 1991; Gibbons *et al.*, 2015) and Burma Block by the Late  
392 Maastrichtian (Socquet and Pubellier, 2005) or the Early Tertiary (Searle *et al.*, 2007) with  
393 southeastern Eurasia.

394 While collision of continental terranes and subduction deactivation events are common phenomenon  
395 in plate tectonics, their relationship to transform boundary migration events is yet unclear (Maia,  
396 2018). Our reconstructions nevertheless provide first order constraints on the context in which the  
397 migration of the India-Africa transform boundary occurred and a way to test the sensitivity of  
398 transform boundary to geodynamic changes. At ~70 Ma, spreading and convergence rates were high  
399 ( $>10 \text{ cm.yr}^{-1}$ ), the age contrast between the adjacent oceanic lithospheres at the Chain Ridge transform  
400 was  $> 30 \text{ Myrs}$ , and the Chain Ridge transform offset was at least of 500-km (Figs. 12, 14). We  
401 propose that the integrated strength of the Chain Ridge transform may have been too high at the time  
402 of this plate reorganization to further accommodate the relative motion of India-Africa, hence resulting  
403 in the relocation of the transform boundary in a weaker area, at the Chain Fracture Zone.

404

## 405 **6- Conclusions**

406

407 Our reconstructions show that during the Late Cretaceous-Late Eocene interval, the India-Africa  
408 transform boundary migrated in response to broader geodynamic events. The Late Maastrichtian  
409 migration from the Chain Ridge Transform to the Chain Fracture Zone records the plate reorganization  
410 event at 74-63 Ma (Cande and Stegman, 2011). The Late Eocene migration from the Chain Fracture to  
411 the present-day location along the Owen Ridge records the well-defined global plate reorganization  
412 event at ~42-47 Ma (Muller *et al.*, 2016). The successive episodes of migration of the India-Africa  
413 plate boundary since the Late Cretaceous contributed to the transfer of oceanic slivers between both  
414 plates. Our updated paleogeographic framework suggests that the lithosphere presently subducting  
415 beneath eastern Makran originates from the East Somali Basin in the Indian Ocean, instead of the  
416 Neotethys as previously proposed.

417 This study also highlights how ophiolites may be emplaced along a transform boundary as a  
418 consequence of a transform migration event. Although the proposed scenario fits with all available  
419 geological constraints, a denser grid of seismic reflection profiles along the east Oman margin is  
420 needed to confirm and describe more precisely the mode of development of the en-échelon marginal  
421 ridges, and the related uplift and dismembering of the Masirah Ophiolitic Belt.



422

423 **Acknowledgements**

424 *Seismic lines were processed using Geocluster software from CGG Veritas. This study was supported*  
425 *by SHOM, Ifremer and INSU-CNRS. We warmly thank the editor D. Wyman, Edwin Gnos and an*  
426 *anonymous reviewer for their very helpful and constructive comments.*

427

428

429 **Figure captions:**

430 **Figure 1:** Structural map of the north western Indian Ocean, showing the currently active plate  
431 boundaries, the distribution of the oceanic basins, as well as the distribution of the main ophiolites.

432 **Figure 2:** General paleogeographic reconstructions of the Indian Ocean from Early Cretaceous to  
433 Early Tertiary, proposed by Gaina *et al.* (2015), and main geological events during the history of the  
434 Indian Ocean. KB: Kabul Block; Masc. : Mascarenes; Sey: Seychelles; GPRE : Global Plate  
435 Reorganization Events.

436 **Figure 3:** a) Free air gravity map of the Owen Basin offshore Oman and the Arabian Sea (filtered for  
437 short wavelengths from DTU 13 database; Andersen *et al.*, 2013) and b) its interpretation,  
438 with an emphasis on the composite age of the basement of the Owen Basin. HNMFS: Haushi-  
439 Nafun-Maradi Fault System.

440 **Figure 4:** a) Free air gravity map of the North Somali Basin (filtered for short wavelengths from DTU  
441 13 database; Andersen *et al.*, 2013) and b) its interpretation, with an emphasis on the composite age of  
442 the basement of the North Somali Basin. c) New interpretation of a vintage seismic line from Bunce  
443 and Molnar (1977) highlighting a major fossil transform fault at the western edge of Chain Ridge,  
444 interpreted as a remnant of the Late Cretaceous India-Africa plate boundary.

445 **Figure 5 :** Multibeam map of the northern termination of the Chain Ridge and Chain Fracture Zone

446 **Figure 6:** a) Map of the Haushi Nafun Maradi Fault system; b) Simplified geological sketchmap of the  
447 Huqf desert highlighting strike-slip offsets related to the Haushi-Nafun fault, after Platel *et al.*, 1992;  
448 c) line drawing of a seismic profile crossing the Maradi fault, highlighting a negative flower structure,  
449 redrawn from Filbrandt *et al.*, 2006.

450 **Figure 7:** a) Seismic line from the OWEN 2 cruise (Rodriguez *et al.*, 2016) crossing the western side  
451 of the Sawqirah Ridge, where the Masirah ophiolites are tilted westwards, in direction of the Oman  
452 platform; b) Seismic line from the OWEN 2 cruise (Rodriguez *et al.*, 2016) crossing the eastern edge  
453 of the Sawqirah Ridge, showing a piece of the Masirah Ophiolite lying in the Owen Basin, and the  
454 unconformity corresponding to the end of the formation of the marginal ridges. c) Cross section of the

455 Oman margin at the latitude of the Sawqirah Ridge (modified from Rodriguez *et al.*, 2016). Three  
456 main angular unconformities can be tracked across the Owen Basin.

457

458 **Figure 8:** Seismic lines from the Owen-2 cruise (Rodriguez *et al.*, 2016) crossing the Owen Basin.

459 **Figure 9 :** Seismic lines from the Owen-2 cruise (Rodriguez *et al.*, 2016) crossing the Owen Basin.

460 **Figure 10 :** Seismic lines from the Owen-2 cruise (Rodriguez *et al.*, 2016) crossing the Owen Basin.

461 These seismic lines highlight the presence of pre-Maastrichtian fanning configurations lying above the  
462 basement of the western part of the Owen Basin, and their absence in its eastern part. The boundary of  
463 the pre-Maastrichtian fanning configurations roughly coincides with the expected location of the fossil  
464 Chain Fracture Zone (according to reconstructions by Royer *et al.*, 2002).

465 **Figure 11:** a) Seismic profile crossing the Masirah ophiolite in the Batain plain (from Beauchamp *et al.*, 1995) and b) its revised interpretation, highlighting the positive flower structure of the Masirah  
466 Ophiolites. See fig. 3 for location.

468 **Figure 12:** Reconstruction of the configuration of the India-Africa plate Boundary at 65-70 Ma and 60  
469 Ma, highlighting the major migration of the transform system occurring at that time.

470 **Figure 13:** Simplified reconstruction of the mode of emplacement of the Masirah ophiolites along  
471 with the development of the en-échelon marginal ridge system offshore Oman. Note that the  
472 emplacement of the ophiolites last over more than 25 Myrs and does not imply any subduction zone.

473 **Figure 14:** Revised paleogeographic reconstructions of the northwestern Indian Ocean, from 90 Ma to  
474 present-day, modified after Matthews *et al.* (2016). These reconstructions highlight the successive  
475 locations of the India-Africa plate boundary: the Chain Ridge Transform from 90 to 65 Ma, the Chain  
476 Fracture Zone from 65 to 47 Ma, in the vicinity of the Owen Ridge since the Oligocene. The main  
477 paleogeographic implications are the East Somali Basin origin of the lithosphere subducting beneath  
478 the eastern Makran, and the disconnection between the India-Africa transform boundary and the  
479 eastern Pakistan ophiolites.

480

481 **References**

482 Agard, P., Jolivet, L., Vrielynck, B., Burov, E., Monié, P., 2007. Plate acceleration: the  
483 obduction trigger? *Earth and planetary science letters* 258, 428-441.

484 Agard, P., Omrani, J., Jolivet, L., Whitechurch, H., Vrielynck, B., Spakman, W., Monié, P.,  
485 Meyer, B., Wortel, R., 2011. Zagros orogeny: a subduction-dominated process, In:  
486 Lacombe, O., Grasemann, B., Simpson, G. (Eds.), *Geodynamic Evolution of the Zagros*.  
487 *Geological Magazine* 692–725.

488 Agard, P., Yamato, P., Soret, M., Prigent, C., Guillot, S., Plunder, A., Dubacq, B., Chauvet,  
489 A., Monié, P., 2016. Plate interface rheological switches during subduction infancy:  
490 control on slab penetration and metamorphic sole formation. *Earth and Planetary Science*  
491 *Letters*, 451, 208-220.

492 Allen, P.A., 2007. The Huqf supergroup of Oman: basin development and context for  
493 Neoproterozoic glaciation. *Earth Science Reviews* 84, 139-185.

494 Allemann, F., 1979. Time of emplacement of the Zhob Valley ophiolites and Bela ophiolites,  
495 Baluchistan (preliminary report) in: *Geodynamics of Pakistan*, Geol. Surv. Pakistan, Spec.  
496 Mem. 215-242.

497 Ali, J.R., Aitchison, J.C., 2008. Gondwana to Asia : Plate tectonics, paleogeography and the  
498 biological connectivity of the Indian sub-continent from the Middle Jurassic through latest  
499 Eocene (166-35 Ma). *Earth Science Reviews* 88, 145-166.

500 Andersen O., Knudsen, P., Kenyon, S., Factor, J., Holmes, S., 2013. The dtu13 global marine  
501 gravity field—first evaluation. Technical report, DTU Space - National Space Institute

502 Anderson, D.L., 2001. Top-down Tectonics? *Science* 293, 2016-2018.

503 Badshah, M. S., Gnos, E., Jan, M. Q., Afridi, M. I., 2000. Stratigraphic and tectonic evolution  
504 of the northwestern Indian plate and Kabul Block, in Khan, M. A., Treloar, P. J., Searle,  
505 M. P., and Jan, M., eds., *Tectonics of the Nanga Parbat Syntaxis and the Western*  
506 *Himalaya*, Geological Society of London Special Publication, 170, 467-475.

507 Barrie, J.V., Conway, K.W., Harris, P.T., 2013. The Queen Charlotte Fault, British Columbia:  
508 seafloor anatomy of a transform fault and its influence on sediment processes. *Geo-Marine*  
509 *Letters* 33, 311-318

510 Barrier, E., Vrielynck, B., 2008. Palaeotectonic maps of the Middle East. Tectono-  
511 sedimentary-palinspastic maps from Late Norian to Pliocene. 14 maps. Paris  
512 CGMW/CCGM

513 Bhattacharya, G.C., Yatheesh, V., 2015. Plate-tectonic evolution of the deep ocean basins  
514 adjoining the western continental margin of India - a proposed model for the early opening  
515 scenario, In: Mukherjee, S. (Ed.), *Petroleum Geoscience: Indian Contexts*. Springer  
516 International Publishing, Switzerland, 1-61.

517 Beauchamp, W. H., Ries, A. C., Coward, M. P., Miles, J.A., 1995. Masirah Graben, Oman : a  
518 hidden Cretaceous rift basin? *American Association of Petroleum Geologists' Bulletin* 79,  
519 864-79.

520 Beck, R.A., Burbank, D.W., Sercombe, W.J., Riley, G.W., Barndt, J.K., Berry, J.R., Afzal, J.,  
521 Khan, A.M., Jurgen, H., Metje, J., Cheema, A., Shafique, N.A., Lawrence, R.D., Khan, A.,  
522 1995. Stratigraphic evidence for an early collision between northwest India and Asia.  
523 *Nature* 373, 55-58

524 Bercovici, D., 2003. The generation of plate tectonics from mantle convection. *Earth*  
525 *Planetary Science Letters* 205, 107-121.

526 Bernard, A., Munsch, M., 2000. Le bassin des Mascareignes et le bassin de Laxmi (océan  
527 Indien occidental) se sont-ils formés à l'axe d'un même centre d'expansion ? *Comptes*  
528 *Rendus de l'Académie des Sciences Paris* 330, 777-783

529 Besse, J., Courtillot, V., 1988. Paleogeographic maps of the continents bordering the Indian  
530 Ocean since the Early Jurassic. *Journal of Geophysical Research* 93, 11791-808.

531 Bouilhol, P., Jagoutz, O., Hanchar, J.M., Dudas, F.O., 2013. Dating the India-Eurasia  
532 collision through arc magmatic records. *Earth and Planetary Science Letters* 366, 163-175.

533 Breton, J.-P., Béchennec, F., Le Métour, J., Moen-Maurel, L., Razin, P., 2004. Eoalpine (Cretaceous)  
534 evolution of the Oman Tethyan continental margin : insights from a structural field study in Jabal  
535 Akhdar (Oman Mountains). *Georabia* 9, 1-18

536 Buckman, S., Aitchinson, J.C., Nutman, A.P., Bennett, V.C., Saktura, W.M., Walsh, J.M.J.,  
537 Kachovich, S., Hidaka, H., 2018. The Spongtang Massif in Ladakh, NW Himalaya: an Early  
538 Cretaceous record of spontaneous, intra-oceanic subduction initiation in the Neotethys. *Gondwana*  
539 *Research* 63, 226-249.

540 Bunce, E.T., Molnar, P., 1977. Seismic reflection profiling and basement topography in the  
541 Somali Basin: possible fracture zones between Madagascar and Africa. *Journal of*  
542 *Geophysical Research* 82, 5305-5311

543 Burg J.P., 2011. The Asia-Kohistan-India collision : review and discussion. D. Brown and  
544 P.D. Ryan (eds), *Arc-Continent Collision, Frontiers in Earth Sciences*, 279-309, doi  
545 10.1007/978-3-540-88558-0\_10

546 Burg, J.P., 2018. Geology of the onshore Makran accretionary wedge: synthesis and tectonic  
547 interpretation. *Earth Science Reviews* 185, 1210-1231.

548 Calvès, G., Schwab, A. M., Huuse, M., Clift, P. D., Gaina, C., Jolley, D., Tabrez, A. R., Inam,  
549 A., 2011. Seismic volcanostratigraphy of the western Indian rifted margin: The pre-Deccan  
550 igneous province, *Journal of Geophysical Research* 116, B01101, doi:  
551 10.1029/2010JB000862.

552 Cande S.C., Stegman, D.R., 2011. Indian and African plate motions driven by the push force  
553 of the Réunion plume head. *Nature* 475, 47-52

554 Cande, S.,C. Patriat, P., 2015. The anticorrelated velocities of Africa and India in the Late  
555 Cretaceous and early Cenozoic. *Geophysical Journal International* 200, 227-243.

556 Carlson, P.R., Bruns, T.R., Plafker, G., 1988. Late Cenozoic offsets on the offshore  
557 connection between the Fairweather and Queen Charlotte faults off southeast Alaska.  
558 *Marine Geology* 85, 89-97.

559 Cassaigneau, C., 1979, Contribution à l'étude des structures Inde-Eurasie. La zone de suture  
560 de Khost dans le Sud-Est de l'Afghanistan, l'obduction Paléocène et la tectonique Tertiaire,  
561 PhD-thesis, 124: Université des Sciences et Techniques du Languedoc, Montpellier

562 Chaubey, A.K., Dymant, J., Bhattacharya, G.C., Royer, J.Y., Srinivas, K., Yatheesh, V., 2002.  
563 Paleogene magnetic isochrons and palaeo-propagators in the Arabian and Eastern Somali  
564 basins, NW Indian Ocean, In: Clift, P.D., Croon, D., Gaedicke, C., Craig, J. (Eds.), *The*  
565 *Tectonic and Climatic Evolution of the Arabian Sea Region*. Geological Society, London,  
566 Special Publication 195, 71-85.

567 Cochran, J. R., 1988. Somali Basin, Chain Ridge, and origin of the northern Somali Basin  
568 gravity and geoid low. *Journal of Geophysical Research* 93, 11985-12008.

569 Coffin, M. F., Pringle, M.S., Duncan, R.A., Gladchenko, T.P., Storey, M., Müller, R.D.,  
570 Gahagan, L.A., 2002. Kerguelen Hotspot magma output since 130 Ma. *Journal of*  
571 *Petrology* 43, 1121-1139.

572 Courtillot, V.E., Renne, P.R., 2003. On the ages of flood basalt events. *Comptes rendus*  
573 *Géoscience* 335, 113-140.

574 Delescluse, M., Montési, L. G. J., Chamot-Rooke, N., 2008. Fault reactivation and selective  
575 abandonment in the oceanic lithosphere. *Geophysical Research Letters* 35, L16312,  
576 doi:10.1029/2008GL035066.

577 DeMets, C., Merkouriev, S., 2016. High-resolution estimates of Nubia-Somalia plate motion  
578 since 20 Ma from reconstructions of the Southwest Indian Ridge, Red Sea and Gulf of  
579 Aden. *Geophys. J. Int.*, 207, 317-322, doi.org/10.1093/gji/ggw276

580 Dilek, Y., Furnes, H., 2014. Ophiolites and their origins. *Elements* 10, 93-100.

581 Dymant, J., 1998. Evolution of the Carlsberg Ridge between 60 and 45 Ma: Ridge  
582 propagation, spreading asymmetry, and the Deccan-Reunion hotspot. *Journal of*  
583 *Geophysical Research* 103, 24067–24084 doi: 10.1029/98JB01759.

584 Eagles, G., Hoang, H.H., 2014. Cretaceous to present kinematics of the Indian, African and  
585 Seychelles plates. *Geophysical Journal International* 196, 1-14

586 Edwards, R.A., Minshull, T. A., White, R. S., 2000. Extension across the Indian–Arabian  
587 plate boundary: the Murray Ridge. *Geophysical Journal International* 142, 461-477.

588 Ellouz Zimmermann, N. et al., 2007, Offshore frontal part of the Makran accretionary prism (Pakistan)  
589 the Chamak Survey, in *Thrust Belts and Foreland Basins: From Fold Kinematics to Hydrocarbon*  
590 *Systems*, edited by O. L. Lacombe et al., pp. 349–364, Springer, Berlin.

591 Filbrandt, J. B., Al-Dhahab, S., Al-Habsy, A., Harris, K., Keating, J., Al-Mahruqi, S., Ozkaya,  
592 S. I., Richard, P. D., Robertson, T., 2006. Kinematic interpretation and structural evolution  
593 of North Oman, Block 6, since the Late Cretaceous and implications for timing of  
594 hydrocarbon migration into Cretaceous reservoirs. *GeoArabia* 11, 97-140.

595 Fournier, M., Petit C., Chamot-Rooke, N., Fabbri, O., Huchon, P., Maillot, B., Lévrier, C.,  
596 2008a. Do ridge-ridge-fault triple junctions exist on Earth? Evidence from the Aden-  
597 Owen-Carlsberg junction in the NW Indian Ocean. *Basin Research* 20, 575-590, doi:  
598 10.1111/j.1365-2117.2008.00356.x

599 Fournier, M., Chamot-Rooke, N., Petit, C., Fabbri, O., Huchon, P., Maillot, B., Lévrier, C.,  
600 2008b. In-situ evidence for dextral active motion at the Arabia-India plate boundary.  
601 *Nature Geoscience* 1, 54-58, doi: 10.1038/ngeo.2007.24.

602 Fournier, M., Chamot-Rooke, N., Petit, C., Huchon, P., Al-Kathiri, A., Audin, L., Beslier, M.-  
603 O., d'Acremont, E., Fabbri, O., Fleury, J.-M., Khanbari, K., Lévrier, C., Leroy, S.,  
604 Maillot B., Merkouriev, S., 2010. Arabia-Somalia plate kinematics, evolution of the Aden-  
605 Owen-Carlsberg triple junction, and opening of the Gulf of Aden. *Journal of Geophysical*  
606 *Research* 115, B04102, doi: 10.1029/2008JB006257



607 Fournier, M., Chamot-Rooke N., Rodriguez, M., Huchon, P., Petit, C., Beslier, M.-O.,  
608 Zaragosi S., 2011. Owen Fracture Zone: the Arabia-India plate boundary unveiled. *Earth*  
609 *and Planetary Science Letters* 302, 247-252, doi:10.1016/j.epsl.2010.12.027.

610 Frizon de Lamotte, D., Raulin, C., Mouchot, N., Wrobel-Daveau, J.-C., Blanpied, C.,  
611 Ringenbach, J.-C., 2011. The southernmost margin of the Tethys realm during the  
612 Mesozoic and Cenozoic : initial geometry and timing of the inversion processes. *Tectonics*  
613 30, TC3002, doi:10.1029/2010TC002691

614 Gaina, C., van Hinsbergen, D.J.J., Spakman, W., 2015. Tectonic interactions between India  
615 and Arabia since the Jurassic reconstructed from marine geophysics, ophiolite geology,  
616 and seismic tomography. *Tectonics* 34, 875-906, doi: 10.1002/2014TC003780.

617 Gibbons, A. D., Whittaker, J. M., Müller, R. D., 2013. The breakup of East Gondwana:  
618 Assimilating constraints from Cretaceous ocean basins around India into a best-fit tectonic  
619 model. *Journal of Geophysical Research Solid Earth* 118, doi:10.1002/jgrb.50079.

620 Gibbons, A.D., Zahirovic, S., Müller, R.D., Whittaker, J.M., Yateesh, V., 2015. A tectonic  
621 model reconciling evidence for the collisions between India, Eurasia and intra-oceanic arcs  
622 of the central-eastern Tethys. *Gondwana Research* 28, 451-492.

623 Glennie, K. W., Boeuf, M. G. A., Hughes-Clark, M. W., Moody-Stuart, M., Pilar, W. F. H.,  
624 and Reinhardt, B. M., 1974, *Geology of the Oman Mountains: Verh. K. Ned. Geol.*  
625 *Mijnbouwkd. Genoot. Ged.*31, 1-423.

626 Gnos, E., Immenhauser, A., Peters, Tj., 1997. Late Cretaceous/early tertiary convergence  
627 between the Indian and Arabian plates recorded in ophiolites and related sediments.  
628 *Tectonophysics* 271, 1-19.

629 Gnos, E. and Perrin, M., 1997. Formation and evolution of the Masirah ophiolite constrained  
630 by paleomagnetic study of volcanic rocks. *Tectonophysics* 253, 53-64.

631 Gnos, E., Khan, M., Mahmood, K., Khan, A. S., Shafique, N. A., and Villa, I. M., 1998, Bela  
632 oceanic lithosphere assemblage and its relation to the Réunion hotspot: *Terra Nova* 10, 90-95.

633 Gnos, E., and Peters, T., 2003, Mantle xenolith-bearing Maastrichtian to Tertiary alkaline  
634 magmatism in Oman.: *Geochemistry, Geophysics, Geosystems* 4, 8620.

635 Guilmette, C., Smit, M.A., van Hinsbergen, D.J.J., Gürer, D., Corfu, F., Charette, B.,  
636 Maffione, M., Rabeau, O., Savard, D., 2018. Forced subduction initiation recorded in the  
637 sole and crust of the Semail Ophiolite of Oman. *Nature geosciences* 11, 688-695.  
638 <https://doi.org/10.1038/s41561-018-0209-2>

639 Hacker, B.R., Mosenfelder, J.L., Gnos, E., 1996. Rapid emplacement of the Oman ophiolite:  
640 thermal and geochronologic constraints. *Tectonics* 15, 1230-1247.

641 Hébert, R., Bezard, R., Guilmette, C., Dostal, J., Wang, C.S., Liu, Z.F., 2012. The Indus-  
642 Yarlung Zangbo ophiolites from Nanga Parbat to Namche Barwa syntaxes, southern  
643 Tibet : first synthesis of petrology, geochemistry, and geochronology with evidences on  
644 geodynamic reconstructions of Neo-Tethys. *Gondwana Research* 22, 377-397

645 Hooper, P., Widdowson, M., Kelley, S., 2010. Tectonic setting and timing of the final Deccan  
646 flood basalt eruptions. *Geology* 38, 839-842

647 Hubert-Ferrari, A., King, G., van der Woerd, J., Villa, I., Altunel, E., Armijo, R., 2009. Long  
648 term evolution of the North Anatolian Fault : new constraints from its eastern termination.  
649 From: VAN HINSBERGEN, D. J. J., EDWARDS, M. A. & GOVERS, R. (eds) *Collision*  
650 *and Collapse at the Africa–Arabia–Eurasia Subduction Zone*. The Geological Society,  
651 London, Special Publications, 311, 133–154. DOI: 10.1144/SP311.5

652 Hutchison, I., Loudon, K. E., White, R.S., von Herzen, R. P., 1981. Heat flow and age of the  
653 Gulf of Oman. *Earth and Planetary Science Letters* 56, 252-262.

654 Immenhauser A., 1996. Cretaceous sedimentary rocks on the Masirah Ophiolite (Sultanate of  
655 Oman): evidence for an unusual bathymetric history. *Journal of the Geological Society of*  
656 *London* 153, 539-551.

657 Immenhauser, A., Schreurs, G., Gnos, E., Oterdoom, H. W., Hartmann, B., 2000. Late  
658 Palaeozoic to Neogene geodynamic evolution of the northeastern Oman margin.  
659 *Geological Magazine* 137, 1-18.

660 Jagoutz, O., Royden, L., Holt, A., Becker, T., 2015. Anomalously fast convergence of India  
661 and Eurasia caused by double subduction. *Nature Geoscience* 8, 475-478.

662 Jolivet, L., Faccenna, C., Agard, P., Frizon de Lamotte, D., Menant, A., Sternai, P., Guillocheau, F.,  
663 2016. Neo-Tethys geodynamics and mantle convection : from extension to compression in Africa  
664 and a conceptual model for obduction. *Canadian Journal of Earth Science* 53, 1190-1204.

665 Kakar, M. I., Kerr, A.C., Mahmood, K., Collins, A.S., Khan, M., McDonald, I., 2014. Supra-  
666 subduction zone tectonic setting of the Muslim Bagh ophiolite, north-western Pakistan: Insights  
667 from geochemistry and petrology. *Lithos* 202-203, 190-206.

668 Khan, S.D., Mahmood, K., Casey, J.F., 2007. Mapping of Muslim Bagh ophiolite complex  
669 (Pakistan) using new remote sensing and field data. *Journal of Asian Earth Sciences* 30,  
670 333-343

671 Kukowski, N., Schillhorn, T., Huhn, K., von Rad, U., Husen, S., Flueh, E.R., 2001.  
672 Morphotectonics and mechanics of the central Makran accretionary wedge off Pakistan.  
673 *Marine Geology* 173, 1-19.

674 Le Pichon, X., A. M. C. Sengor, J. Kende, C. Imren, P. Henry, C. Grall, H. Karabulut, 2016.  
675 Propagation of a strike-slip plate boundary within an extensional environment: the  
676 westward propagation of the North Anatolian Fault. *Canadian Journal of Earth Sciences*  
677 53, 1416-1439, <https://doi.org/10.1139/cjes-2015-0129>

678 Mahanjane, E.S., 2014. The Davie Fracture Zone and adjacent basins in the offshore  
679 Mozambique Margin-A new insights for the hydrocarbon potential. *Marine and Petroleum*  
680 *Geology* 57, 561-571.

681 Mahmood, K., Boudier, F., Gnos, E., Monié, P., Nicolas, A., 1995.  $^{40}\text{Ar}/^{39}\text{Ar}$  dating of the  
682 emplacement of the Muslim Bagh ophiolite, Pakistan. *Tectonophysics* 250, 169-181

683 Maia, M., S. Sichel, A. Briais, D. Brunelli, M. Ligi, N. Ferreira, T. Campos, B. Mougel, I.  
684 Brehme, C. Hémond, A. Motoki, D. Moura, C. Scalabrin, I. Pessanha, E. Alves, A. Ayes,  
685 and P. Oliveira (2016). Extreme mantle uplift and exhumation along a transpressive  
686 transform fault, *Nat. Geosci.*, DOI:10.1038/NGEO2759

687 Matthews, K. J., Seton, M., Müller, R., 2012. A global-scale plate reorganization event at 105-100 Ma.  
688 *Earth and Planetary Science Letters* 355-356, 283-298.

689 Matthews, K.J., Müller, R.D., Sandwell, D.T., 2015. Oceanic microplate formation records  
690 the onset of India-Eurasia collision. *Earth and Planetary Science Letters*, 433, 204-214,  
691 doi:10.1016/j.epsl.2015.10.040

692 Matthews, K.J., Maloney, K.T., Zahirovic, S., Williams, S.E., Seton, M., Müller, D.R., 2016.  
693 Global plate boundary evolution and kinematics since the late Paleozoic. *Global and*  
694 *Planetary Change* 146, 226-250.

695 McCall, G.J.H., 1997. The geotectonic history of the Makran and adjacent areas of southern  
696 Iran. *Journal of Asian Earth Sciences* 15, 517-531.

697 Meckel, T.A., Coffin, M.F., Mosher, S., Symonds, P., Bernadel, G., Mann, P., 2003.  
698 Underthrusting at the Hjort Trench, Australian-Pacific plate boundary: incipient  
699 subduction? *Geochemistry, Geophysics, Geosystems* 12, doi:10.1029/2002GC000498

700 Merkouriev, S., Patriat, P., Sochevanova, N., 1996. Evolution de la dorsale de Carlsberg:  
701 Evidence pour une phase d'expansion très lente entre 40 et 25 Ma (A18 à  
702 A7). *Oceanologica Acta* 19, 1-13.

703 Minshull, T.A., Lane, C., Collier, J. S., Whitmarsh, R., 2008. The relationship between rifting  
704 and magmatism in the northeastern Arabian Sea. *Nature Geoscience* 1, 463-467,  
705 doi:10.1038/ngeo228

706 Molnar, P., Stock, J., 2009. Slowing of India's convergence with Eurasia since 20 Ma and its  
707 implications for Tibetan mantle dynamics. *Tectonics* 28, TC3001, doi:  
708 10.1029/2008TC002271

709 **MORRIS 2017**

710 Mouchot, N. 2009. Tectonique et sédimentation sur le complexe de subduction du Makran  
711 pakistanais. PhD thesis, Univ. Cergy Pontoise, 208 pp.

712 Mountain, G. S., Prell, W. L., 1990. A multiphase plate tectonic history of the southeast  
713 continental margin of Oman, *The Geology and Tectonics of the Oman Region*, edited by  
714 Robertson, A. H. F., Searle, M. P. and Ries, A. C. Geological Society Special Publication  
715 49, 725-743.

716 Müller, R.D., Seton, M., Zahirovic, S., Williams, S.E., Matthews, K.J., Wright, N.M., Shepard, G.E.,  
717 Maloney, K.T., Barnett-Moore, N., Hosseinpour, M., Bower, D.J., Cannon, J., 2016. Ocean Basin  
718 evolution and global-scale plate reorganization events since Pangea Breakup. *Annual Review of*  
719 *Earth and Planetary Sciences* 44, 107-138, <https://doi.org/10.1146/annurev-earth-060115-012211>

720 Nicolas, A. and Boudier, F., 2017. Emplacement of Semail-Emirates ophiolite at ridge-trench  
721 collision. *Terra Nova* 29, 127-134

722 Norton, I.O., Sclater, J.G., 1979. A model for the evolution of the Indian Ocean and the break-  
723 up of Gondwanaland. *Journal of Geophysical Research* 84, 6803-6830.

724 Patriat, P., Achache, J., 1984. India-Eurasia collision chronology has implications for crustal  
725 shortening and driving mechanism of plate. *Nature* 311, 615-621.

726 Patriat, P., Sloan, H., Sauter, D., 2008. From slow to ultraslow: a previously undetected event  
727 at the Southwest Indian Ridge at ca. 24 Ma. *Geology* 36, 207-210, doi: 10.1130/G24270A.1

728 Peters, Tj., Mercolli, I., 1998. Extremely thin oceanic crust in the Proto-Indian Ocean:  
729 Evidence from the Masirah Ophiolite, Sultanate of Oman. *Journal of Geophysical Research*  
730 103, 677-689.

731 Platel, J. P., A. Berthiaux, J. Le Métour, M. Beurrier, J. Roger (1992), Geological map of  
732 Duqm and Madraka, Sultanate of Oman, sheet NE 40-03/07, scale 1: 250000, Oman  
733 Minist. of Pet. and Miner., Dir. Gen. of Miner., Muscat.

734 Pubellier, M., Girardeau, J., Tjashuri, J., 1999. Accretion history of Borneo inferred from the  
735 polyphase structural features in the Meratus Mountains. In: Metcalfe (Ed.), *Gondwana*  
736 *Dispersion and Asian Accretion-Final results of IGCP 321*. AA Balkema Publishers,  
737 Rotterdam, 141-160. Ravaut, P., Bayer, R., Hassani, R., Rousset, P., and Al-Yahya-ey, A., 1997,  
738 Structure and evolution of the northern Oman margin; gravity and seismic constraints over the  
739 Zagros-Makran-Oman collision zone: *Tectonophysics* 279, 253-280.

740 Ravaut, P., Carbon, D., Ritz, J.F., Bayer, R., Philip, H., 1998. The Sohar Basin, Western Gulf of  
741 Oman : description and mechanisms of formation from seismic and gravity data. *Marine and*  
742 *Petroleum Geology* 15, 359-377.

743 Robinet, J., Razin, P., Serra-Kiel, J., Gallardo-Garcia, A., Leroy, S., Roger, J., Grelaud, C.,  
744 2013. The Paleogene pre-rift to syn-rift succession in the Dhofar margin (northeastern gulf  
745 of Aden): stratigraphy and depositional environments. *Tectonophysics* 607, 1-16.

746 Rodriguez, M., Fournier, M., Chamot-Rooke, N., Huchon, P., Bourget, J., Sorbier, M.,  
747 Zaragosi, S., Rabaute, A., 2011. Neotectonics of the Owen Fracture Zone (NW Indian  
748 Ocean): structural evolution of an oceanic strike-slip plate boundary. *Geochemistry*  
749 *Geophysics Geosystems* 12, doi:10.1029/2011GC003731.

750 Rodriguez, M., Chamot-Rooke, N., Fournier, M., Huchon, P., Delescluse, M., 2013. Mode of  
751 opening of an oceanic pull-apart: The 20 °N Basin along the Owen Fracture Zone (NW  
752 Indian Ocean). *Tectonics* 32, 1-15, doi:10.1002/tect.20083.

753 Rodriguez, M., Chamot-Rooke, N., Huchon, P., Fournier, M., Delescluse, M., 2014a. The

754 Owen Ridge uplift in the Arabian Sea: implications for the sedimentary record of Indian  
755 monsoon in Late Miocene. *Earth and Planetary Science Letters* 394, 1-12, doi:  
756 10.1016/j.epsl.2014.03.011

757 Rodriguez, M., Chamot-Rooke, N., Huchon, P., Fournier, M., Lallemand, S., Delescluse, M.,  
758 Zaragosi, S., Mouchot, N., 2014b. Tectonics of the Dalrymple Trough and uplift of the  
759 Murray Ridge (NW Indian Ocean). *Tectonophysics*, 636, 1-17, doi:  
760 10.1016/j.tecto.2014.08.001

761 Rodriguez, M., Huchon, P., Chamot-Rooke, N., Fournier, M., Delescluse, M., François, T.  
762 2016. Tracking the Paleogene India-Arabia plate boundary. *Marine and Petroleum*  
763 *Geology*, 72, 336-358, doi:10.1016/j.marpetgeo.2016.02.019

764 Rodriguez, M., Fournier, M., Chamot-Rooke, N., Huchon, P., Delescluse, M., 2018. The  
765 geological evolution of the Aden-Owen-Carlsberg triple junction (NW Indian Ocean) since  
766 the Late Miocene, *Tectonics*, 37, 1552-1575, <https://doi.org/10.1029/2017TC004687>

767 Rohr, K.M.M., 2015. Plate Boundary Adjustments of the Southernmost Queen Charlotte  
768 Fault. *Bulletin of the Seismological Society of America*, 105, doi:10.1785/0120140162

769 Rollinson, H., 2017. Masirah-The other Oman ophiolite: a better analogue for mid-ocean  
770 ridge processes? *Geoscience Frontiers* 8, 1253-1262

771 Royer, J. Y., Chaubey, A. K., Dymant, J., Bhattacharya, G. C., Srinivas, K., Yateesh, V.,  
772 Ramprasad, T., 2002. Paleogene plate tectonic evolution of the Arabian and Eastern  
773 Somali basins, in *The Tectonic and Climatic Evolution of the Arabian Sea Region*, edited  
774 by P. D. Clift et al., *Geological Society Special Publication* 195, 7-23.

775 Sarwar, G., 1992. Tectonic setting of the Bela Ophiolites, southern Pakistan. *Tectonophysics*  
776 207, 359-381.

777 Searle, M., Cox, J., 1999. Tectonic setting, origin, and obduction of the Oman ophiolite,  
778 *Geological Society of America bulletin* 111, 104-122.

779 Searle, M.P., Noble, S.R., Cottle, J.M., Waters, D.J., Mitchell, A.H.G., Tin Hlaing,  
780 Horstwood, M.S.A., 2007. Tectonic evolution of the Mogok metamorphic belt,  
781 Burma(Myanmar) constrained by U-Th-Pb dating of metamorphic and magmatic rocks.  
782 *Tectonics* 26, TC3014, doi:10.1029/2006TC002083

783 Seton, M., Müller, R.D., Zahirovic, S., Gaina, C., Torsvik, T., Shepard, G., Talsma, A.,  
784 Gurnis, M., Turner, M., Maus, S., Chandler, M., 2012. Global continental and ocean basin  
785 reconstructions since 200 Ma. *Earth Sciences Reviews* 113, 212-270,  
786 doi:10.1016/j.earscirev.2012.03.002.

787 Shackleton, R. M., Ries, A. C., 1990. Tectonics of the Masirah fault zone and eastern Oman.  
788 In *The Geology and Tectonics of the Oman Region*, eds A. H. F. Robertson, M. P. Searle,  
789 and A. C. Ries. Geological Society Special Publication 49, 715-24.

790 Schlich, R., 1982. The Indian Ocean: aseismic Ridges, spreading centres and basins, In:  
791 Nairn, A.E.M., Stehli, F.G. (Eds.), *The Ocean Basins and Margins*. Plenum Press, New  
792 York, 51-147.

793 Schreurs, G., Immenhauser, A., 1999. West-northwest-directed obduction of the Batain group  
794 on the eastern Oman continental margin at the Cretaceous-Tertiary boundary. *Tectonics*  
795 18, 148-60.

796 Shipboard Scientific Party, 1974a. Site 235, In: Fisher, R.L., Bunce, E.T. et al., DSDP  
797 Init.Repts, leg 24. doi:10.2973/dsdp.proc.24.1974

798 Shipboard Scientific Party 1974b, Site 222. In: Whitmarsh, R.B., Weser, O.E., Ross, D.A.  
799 (Eds.), DSDP Init. Repts, leg 23 <http://dx.doi.org/10.2973/dsdp.proc.23.106>.

800 Shipboard Scientific Party 1989, Site 731. In: Prell, W.L., Niitsuma, N., et al. (Eds.), Proc.  
801 ODP, Init.Repts., 117. College Station, TX (Ocean Drilling Program).

802 Socquet, A., Pubellier, M., 2005. Cenozoic deformation in Western Yunnan (China-Myanmar  
803 border), *Journal of Asian Earth Sciences*, 24, 495-511



804 Smit, J., Brun, J.-P., Cloething, S., Ben Avraham, Z., 2010. The rift like structure and asymmetry of  
805 the Dead Sea Fault. *Earth and Planetary Science Letters* 290, 74-82.

806 Tapponnier, P., Mattauer, M., Proust, F., Cassaigneau, C., 1981. Mesozoic ophiolites, sutures,  
807 and large-scale tectonic movements in Afghanistan. *Earth and Planetary Science Letters*  
808 52, 355-371.

809 Tréhu, A.M., Scheidhauer, M., Rohr, K.M.M., Tikoff, B., Walton, M.A., Gulick, S.P.S.,  
810 Roland, E., 2015. An abrupt transition in the mechanical response of the upper crust to  
811 transpression along the Queen Charlotte Fault, *Bulletin of the Seismological Society of*  
812 *America*, 105, doi:10.1785/0120159.

813 Treolar, P.J., Izatt, C.N., 1993. Tectonics of the Himalayan collision between the Indian Plate  
814 and the Afghan Block: a synthesis. *Geological Society Special Publication*, 74, 69-87

815 van Hinsbergen, D.J.J., Steinberger, B., Doubrovine, P.V., Gassmüller, R., 2011. Acceleration  
816 and deceleration of India-Asia convergence since the Cretaceous: Roles of mantle plumes  
817 and continental collision. *Journal of Geophysical Research*, 116, B06101,  
818 doi:10.1029/2010JB0085051

819 van Hinsbergen, D. J. J., Lippert, P. C., Dupont-Nivet, G., McQuarrie, N., Doubrovine, P. V.,  
820 Spakman W., Torsvik, T. H., 2012. Greater India Basin hypothesis and a two-stage  
821 Cenozoic collision between India and Asia. *Proceedings of the National Academy of*  
822 *Sciences* 109, 7659-7664.

823 Wajzer, M.R., Barber, A.J., Hidayat, S., Suharsono, S., 1991. Accretion, collision and strike-  
824 slip faulting: the Woyla group as a key to the tectonic evolution of North Sumatra. *Journal*  
825 *of Southeast Asian Earth Sciences*, 6, 447-461

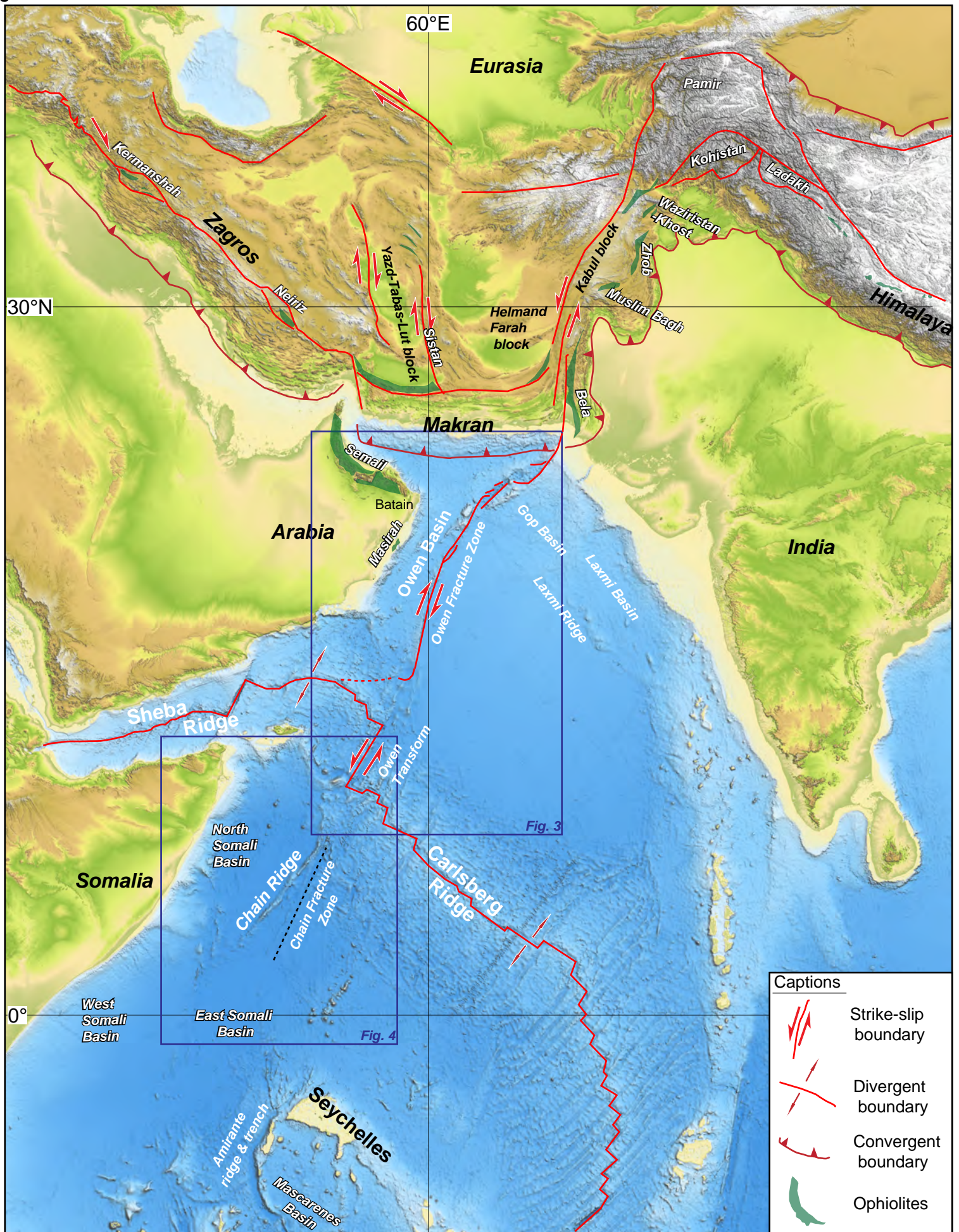
826 Wakabayashi, J., Dilek, Y., 2003. What constitutes ‘emplacement’ of an ophiolite?  
827 Mechanisms and relationship to subduction initiation and formation of metamorphic soles.  
828 *Geological Society of London, Special publications*, 218, 427-447.  
829 <https://doi.org/10.1144/GSL.SP.2003.218.01.22>

830 Wyns, R., Béchenec, F., Le Métour, J., Roger, J., and Chevrel, S., 1992, Explanatory notes,  
831 Geological map of Sur, sheet NF 40-08, scale 1:250'000, Muscat, Sultanate of Oman,  
832 Ministry of Petroleum and Minerals, 1-103

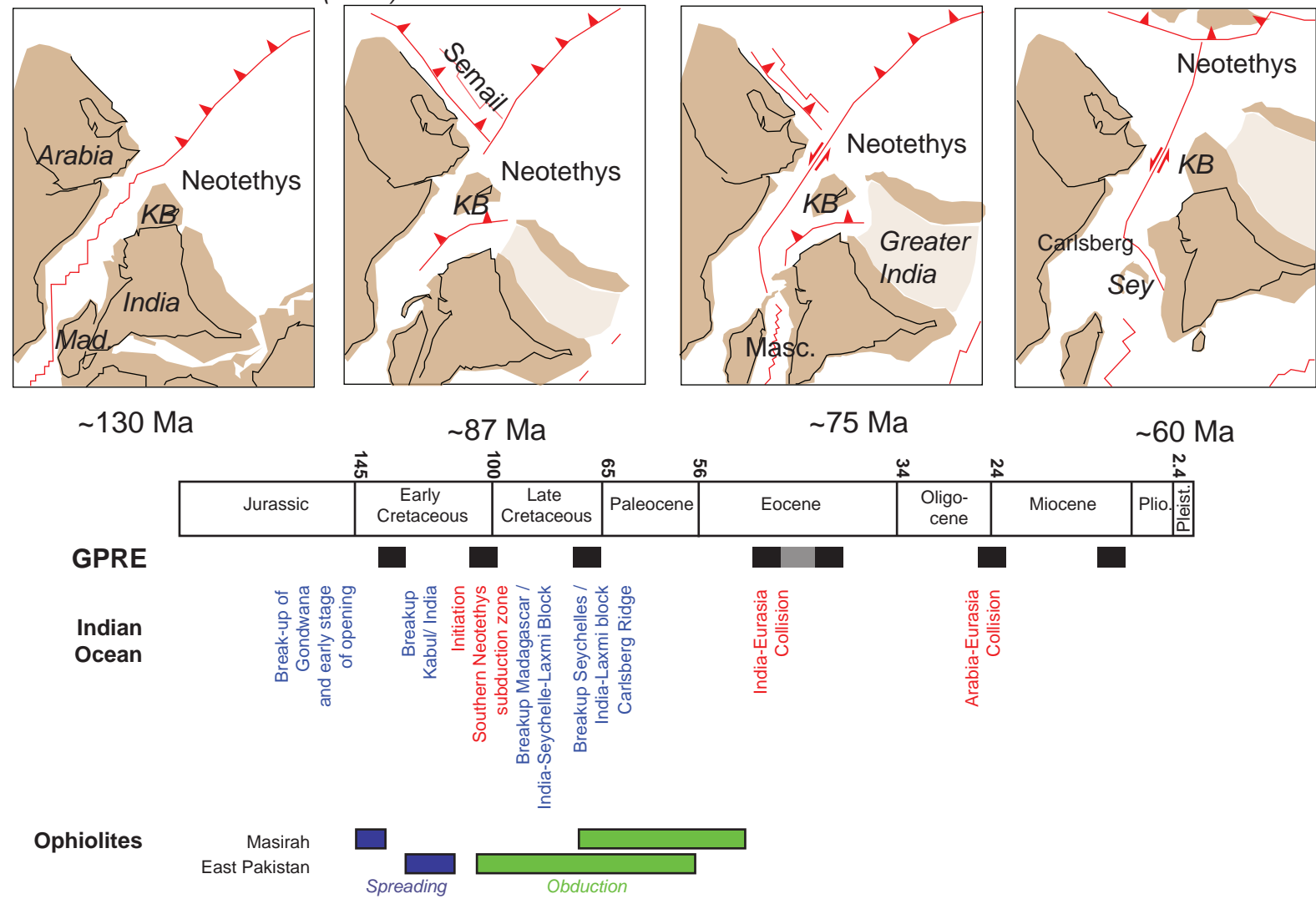
833 Yateesh, V., Bhattacharya, G. C., Dymant, J., 2009. Early oceanic opening off Western India-  
834 Pakistan margin : the Gop Basin revisited. *Earth and Planetary Science Letters* 284, 399-  
835 408.

836 Zhuang, G., Najman, Y., Guillot, S., Roddaz, M., Antoine, P.-O., Métais, G., Carter, A.,  
837 Marivaux, L., Solangi, S.H., 2015. Constraints on the collision and the pre-collision  
838 tectonic configuration between India and Asia from detrital geochronology,  
839 thermochronology, and geochemistry studies in the lower Indus basin, Pakistan. *Earth and*  
840 *Planetary Science Letters* 432, 363-373.

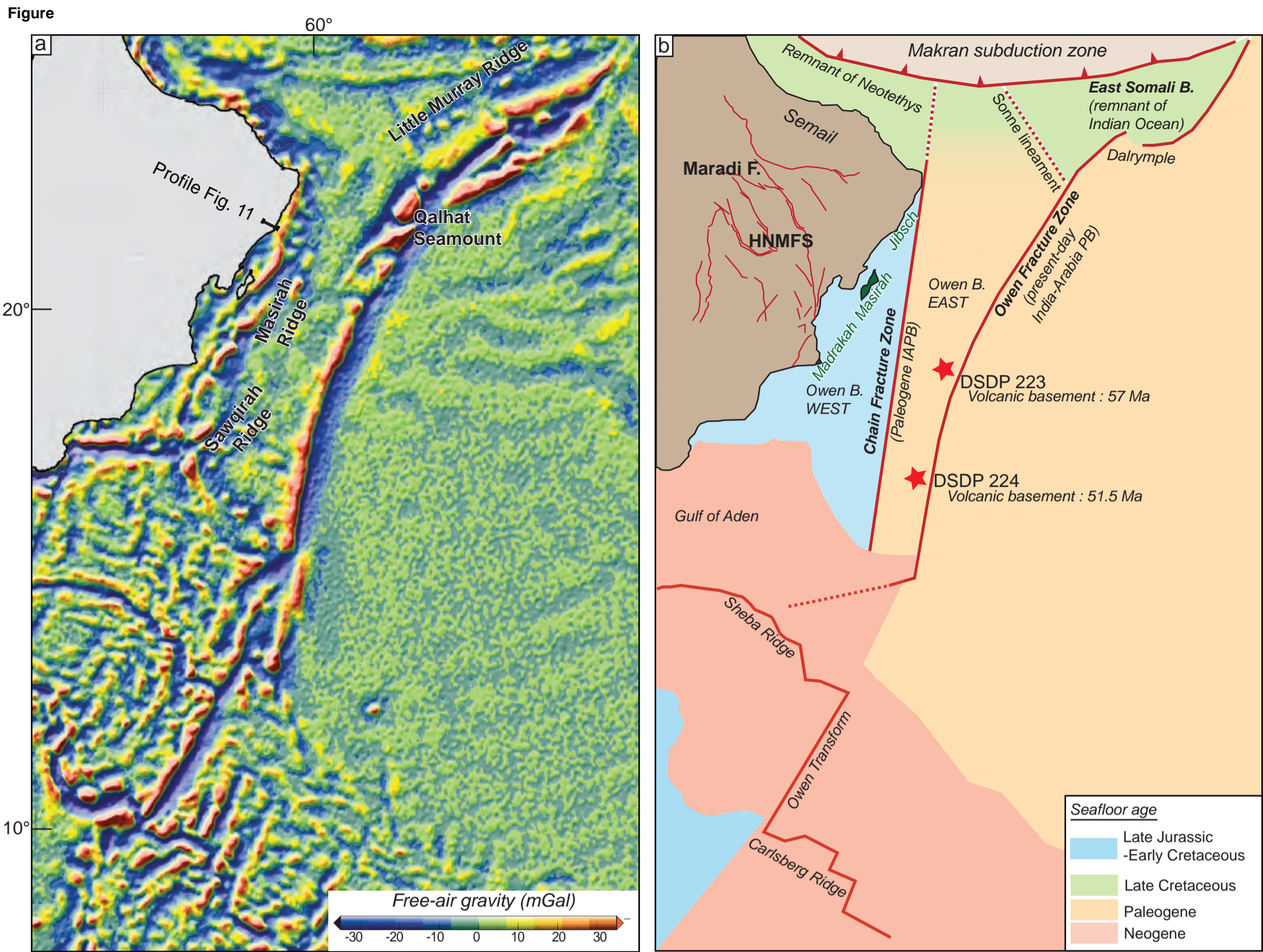
Figure

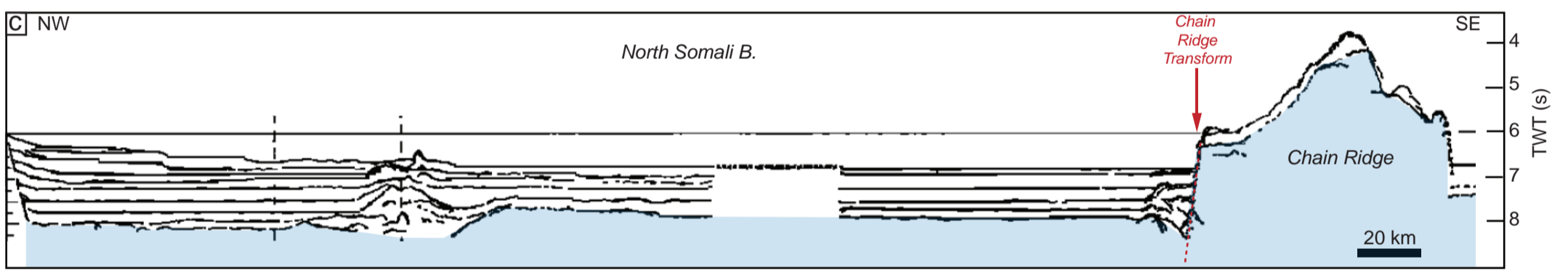
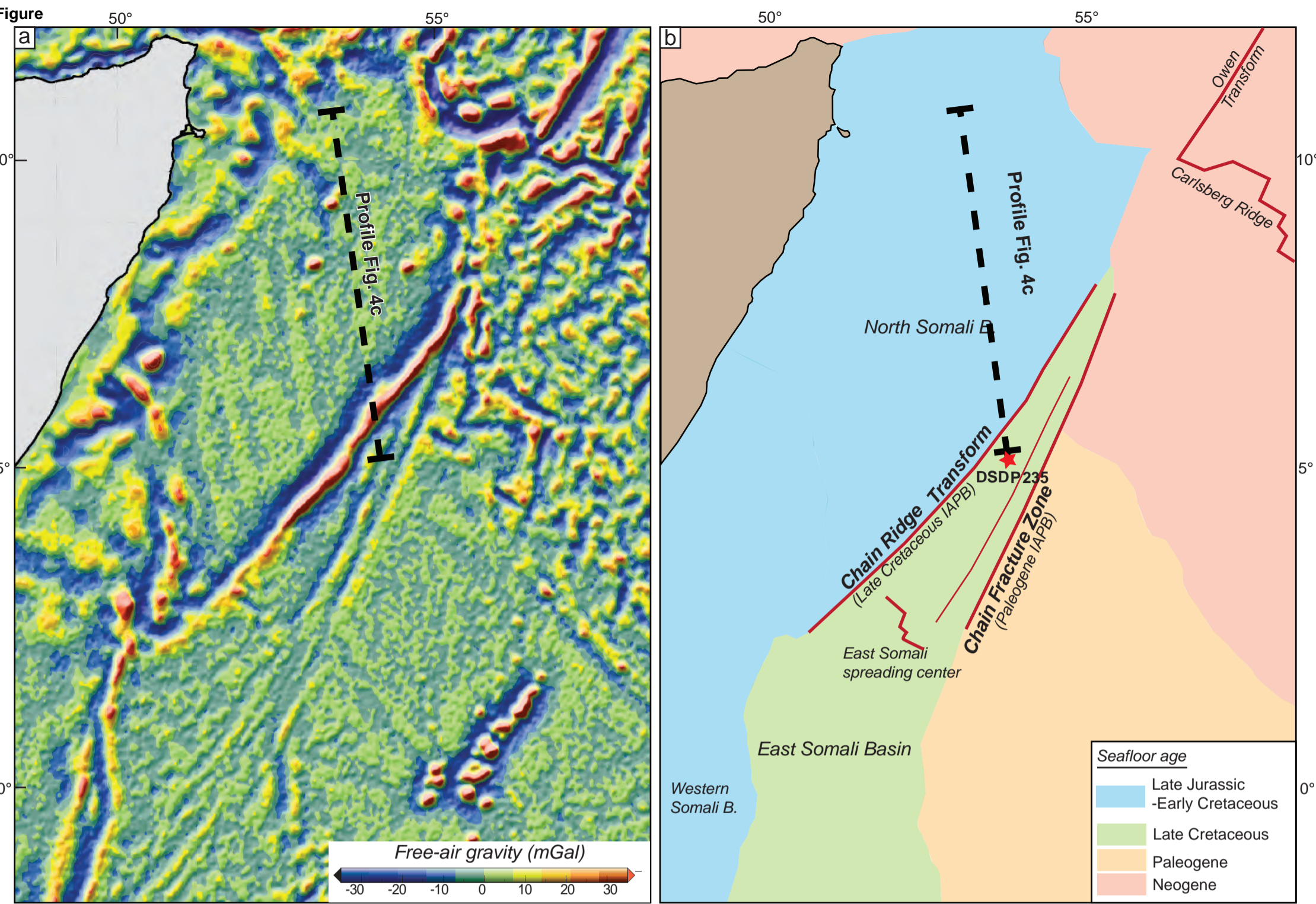


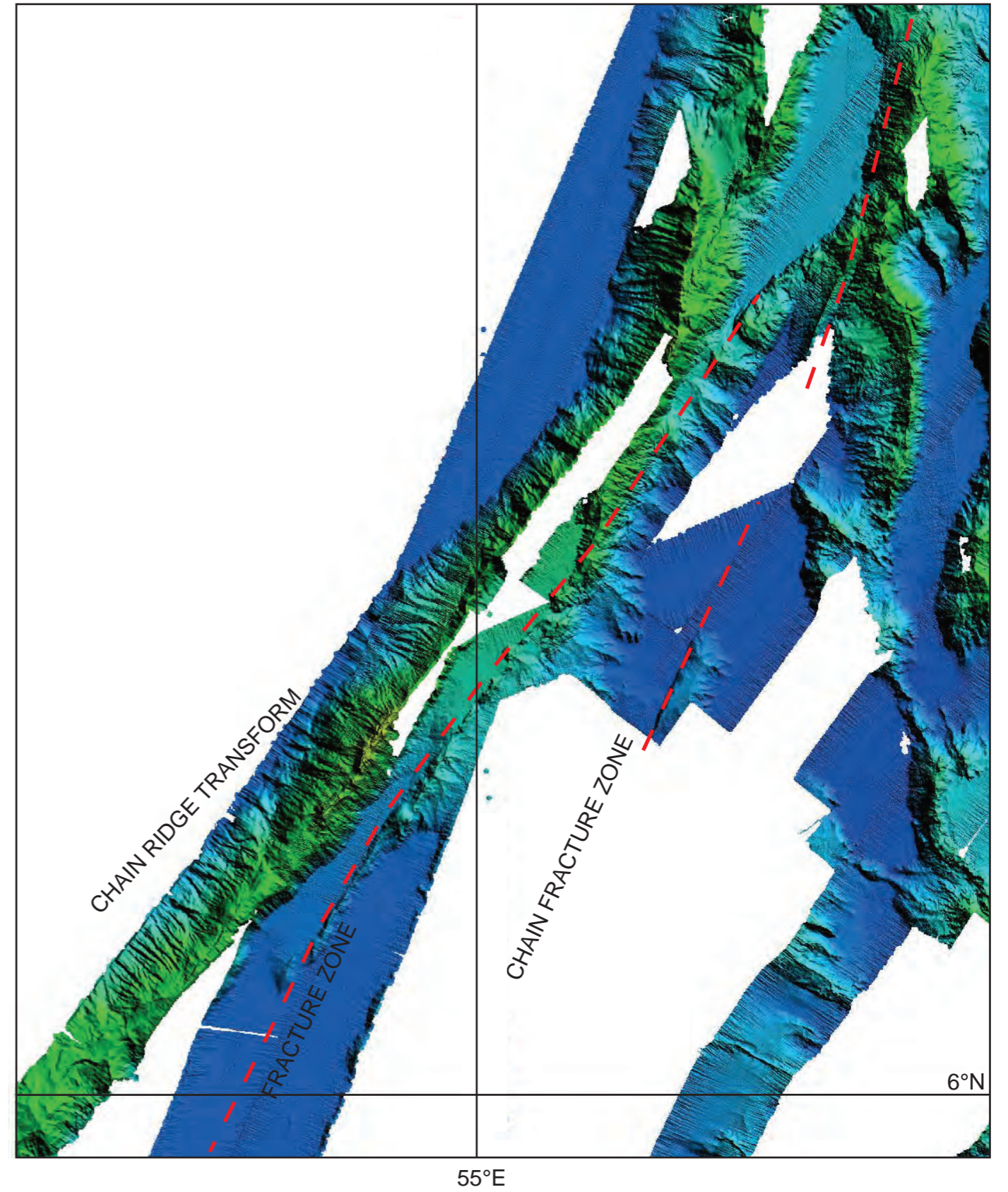
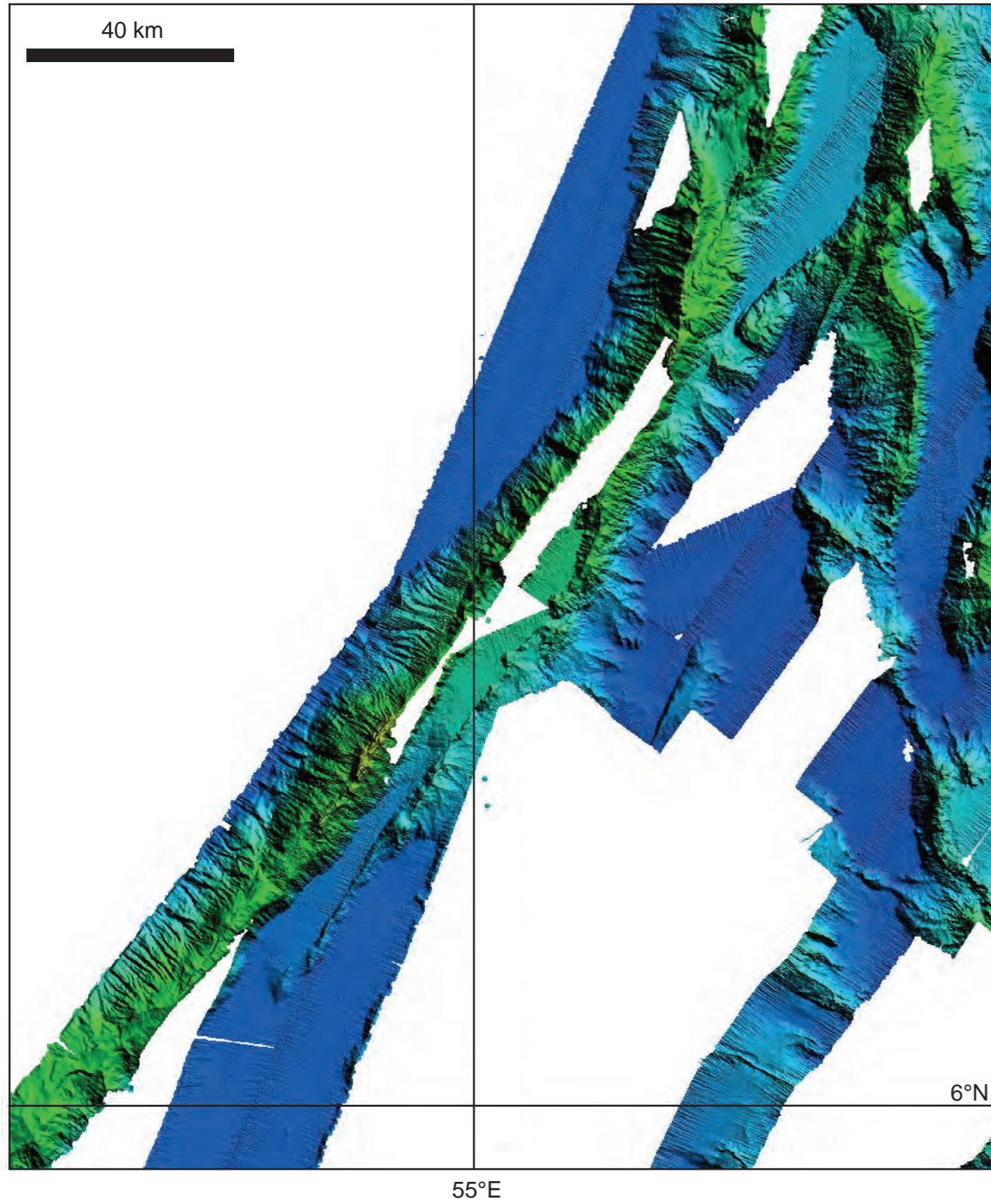
Modified from Gaina et al. (2015)

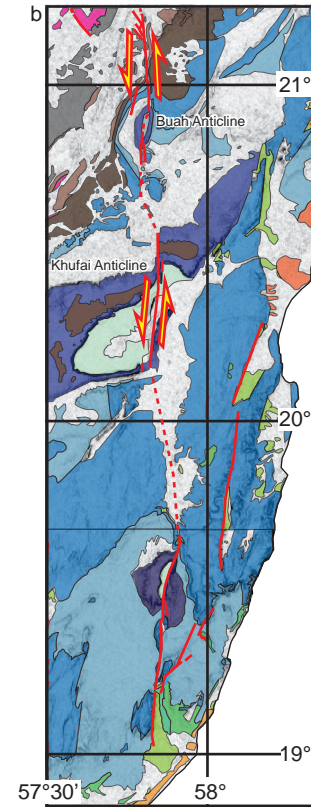
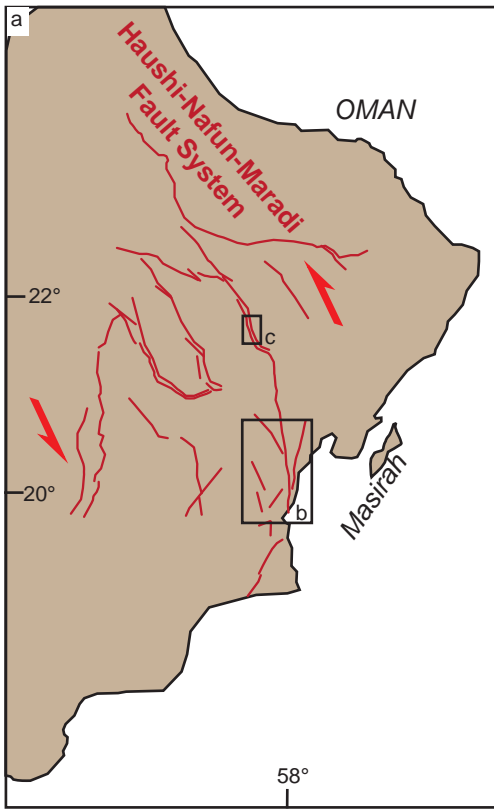


Figure

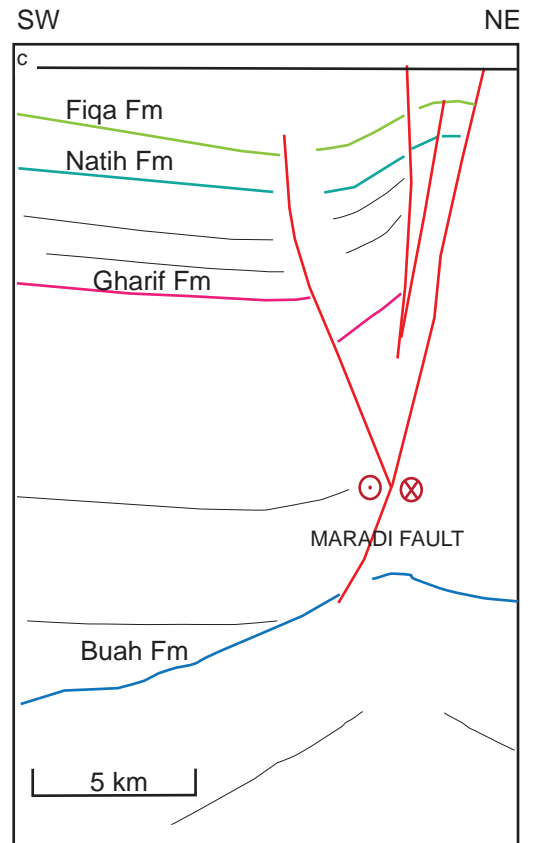




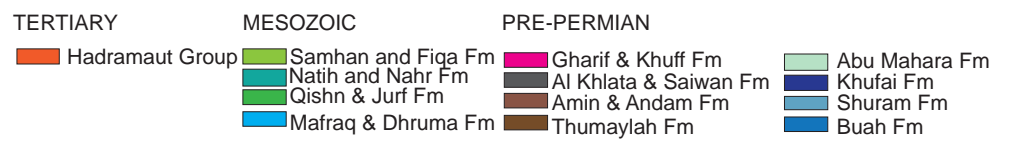




Modified from Platel et al., 1992

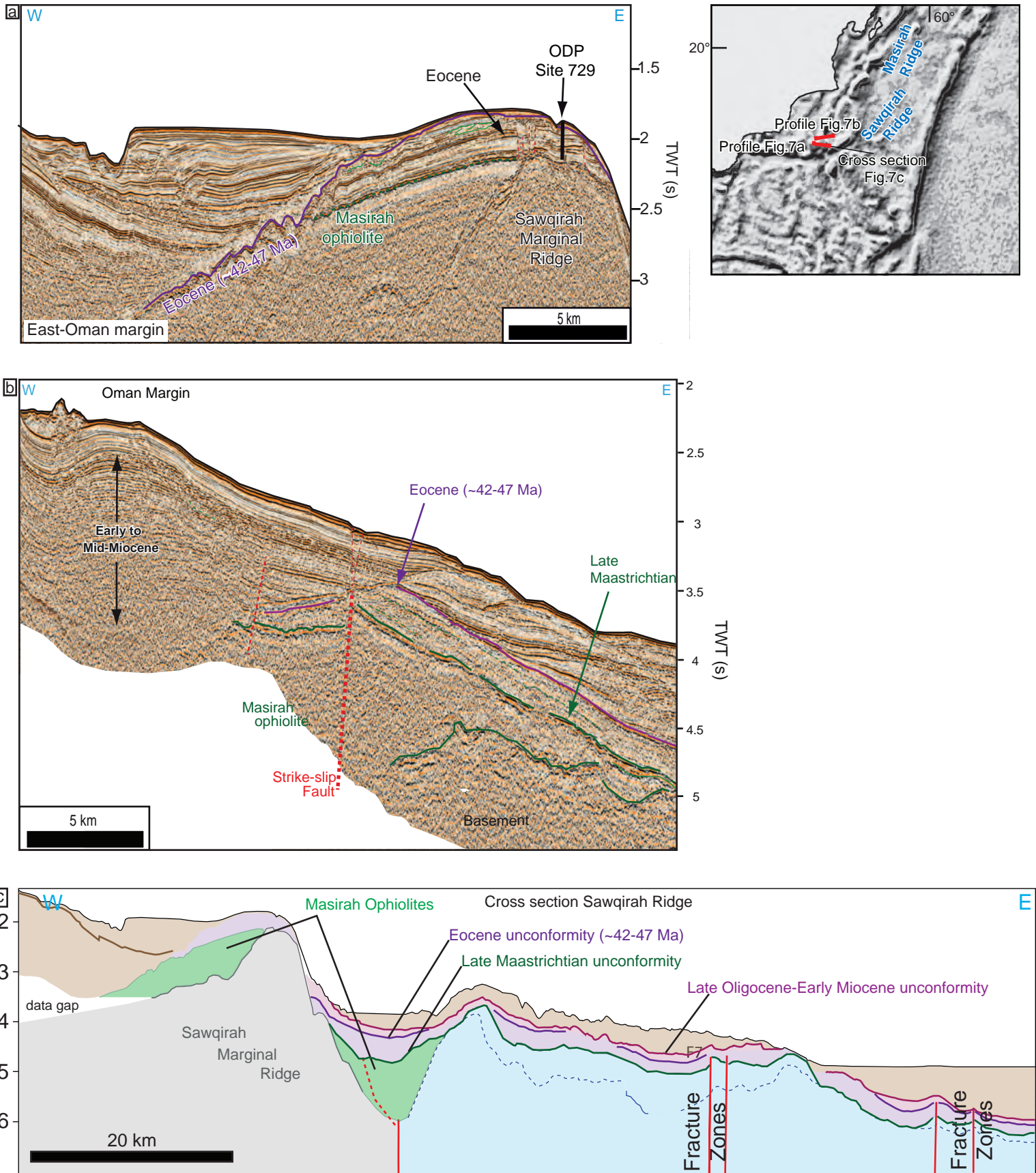


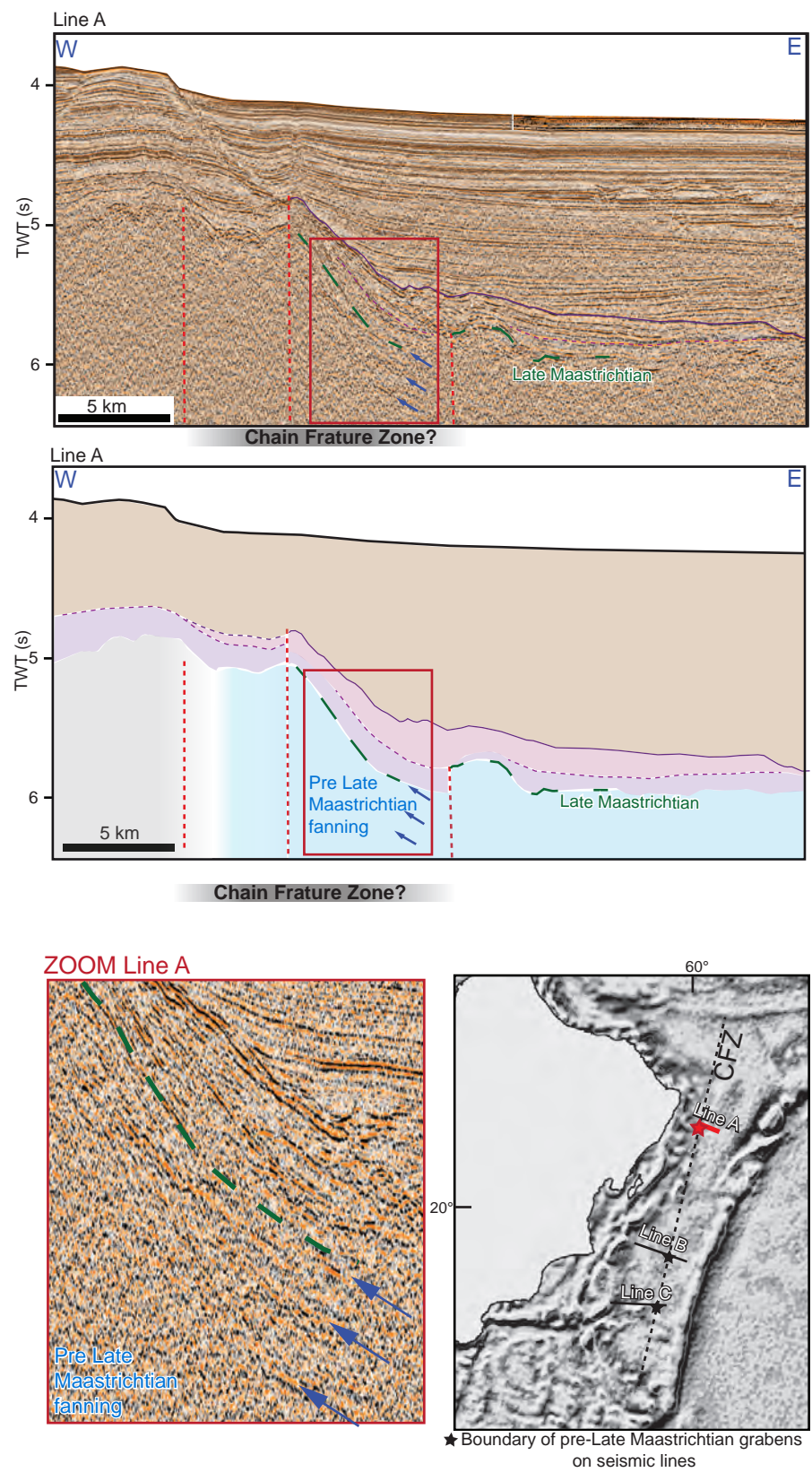
Modified from Filbrandt et al., 2006





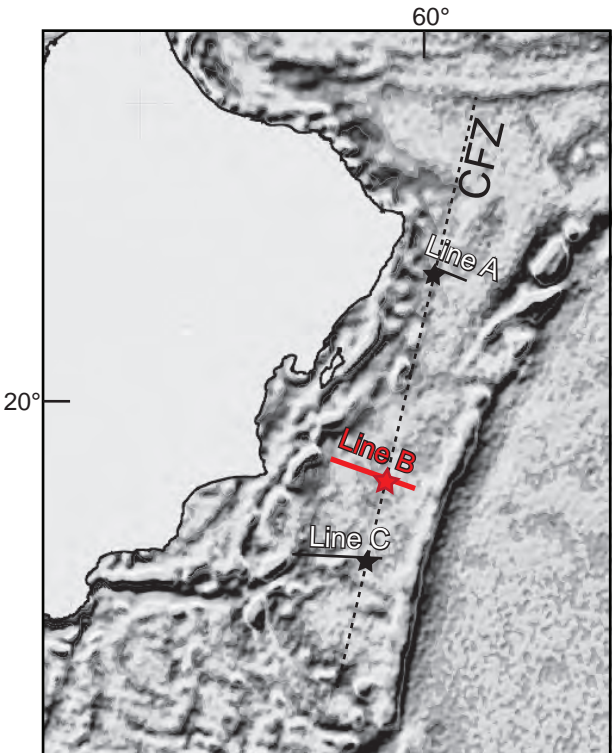
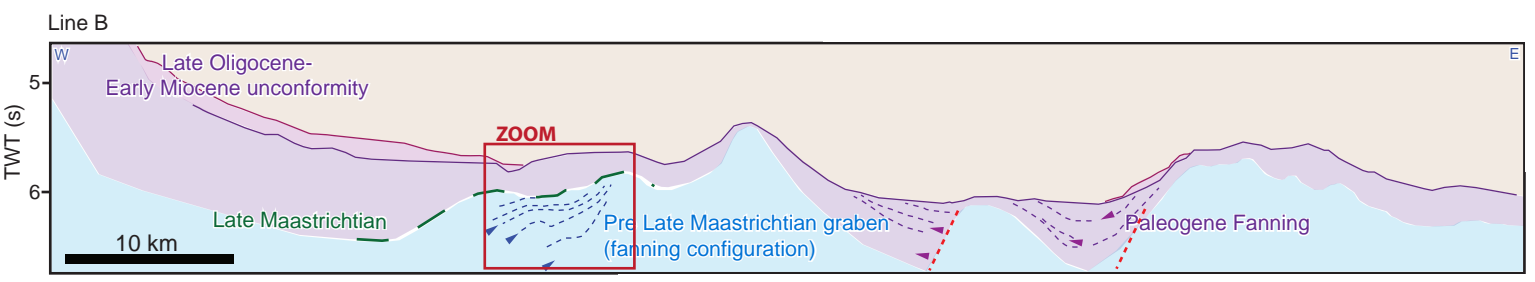
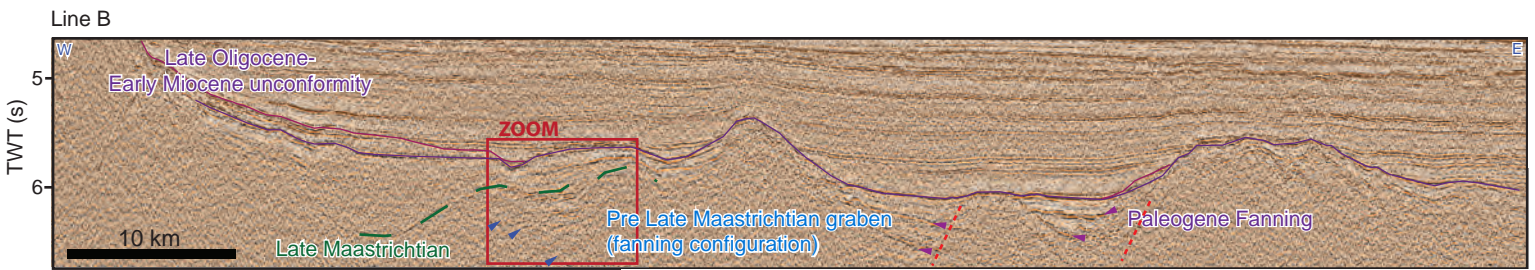
Figure





★ Boundary of pre-Late Maastrichtian grabens on seismic lines

Figure



★ Boundary of pre-Late Maastrichtian grabens on seismic lines

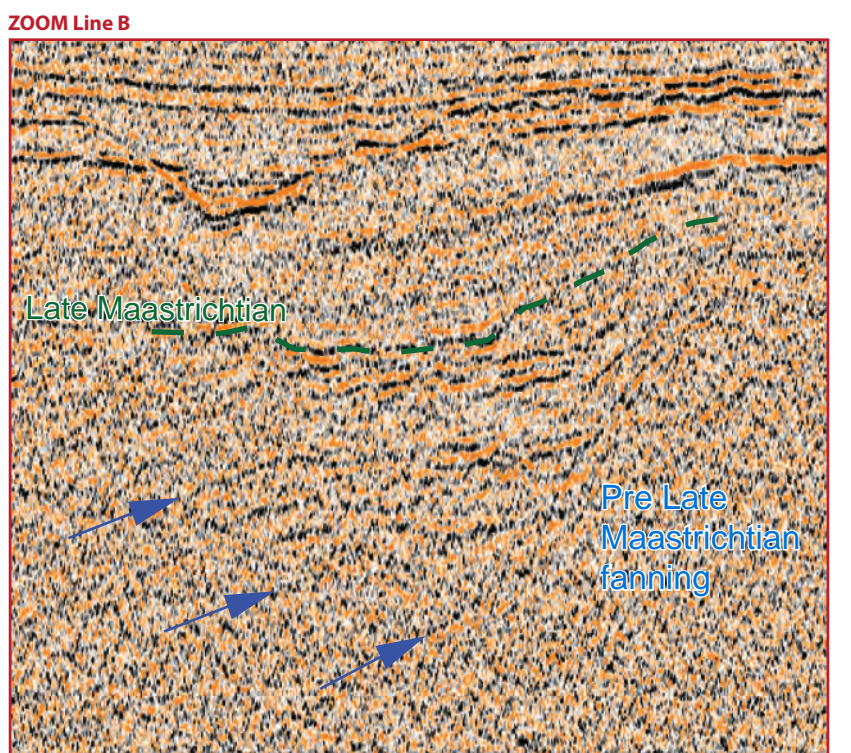
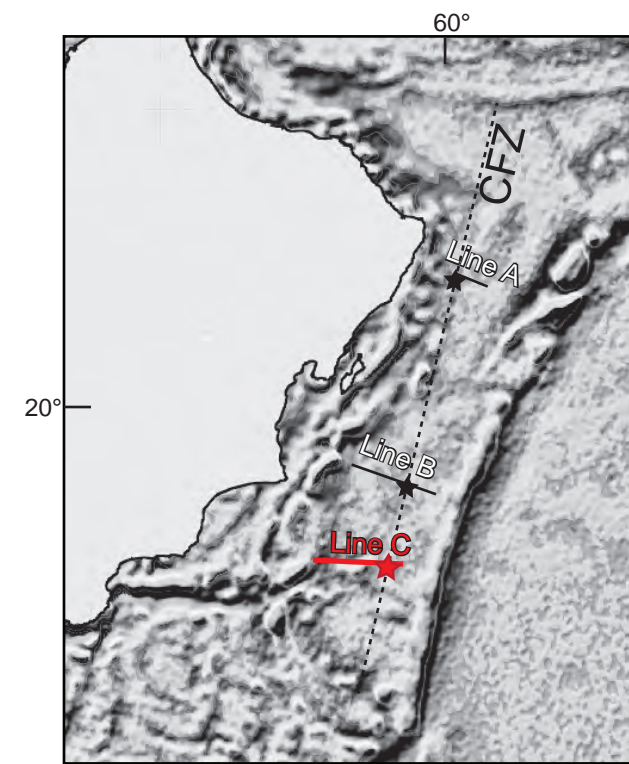
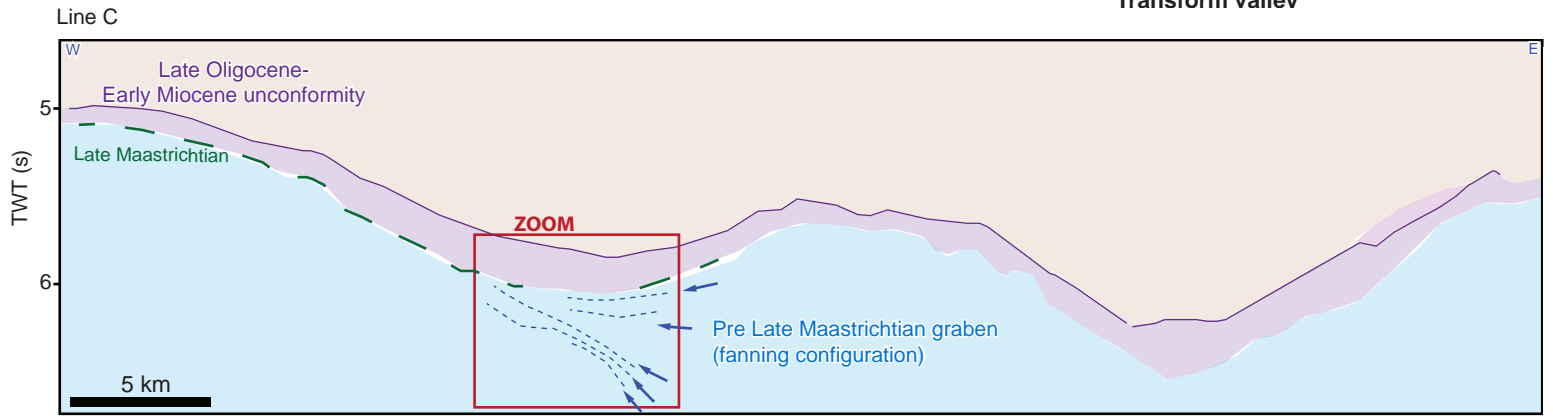
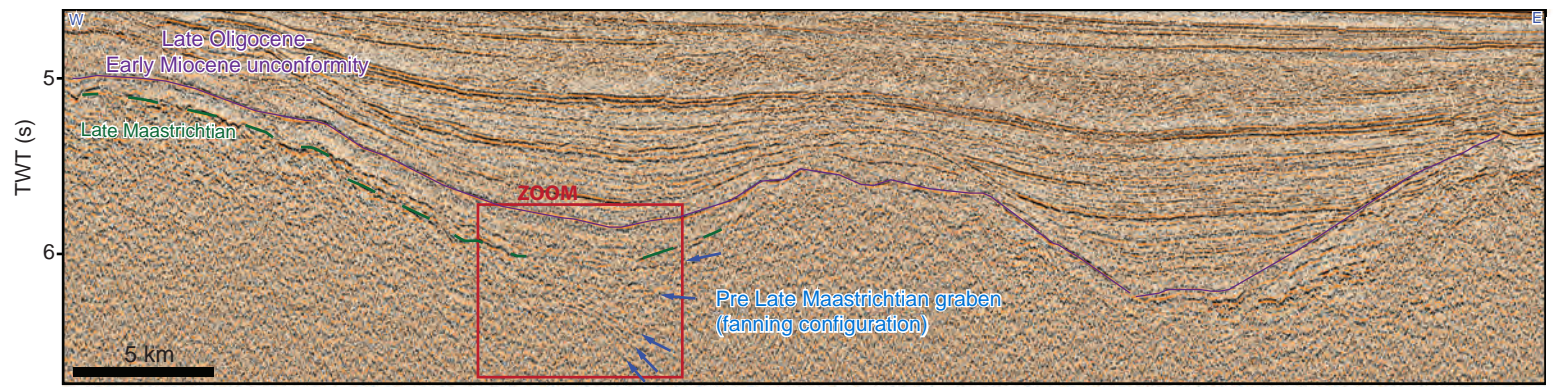
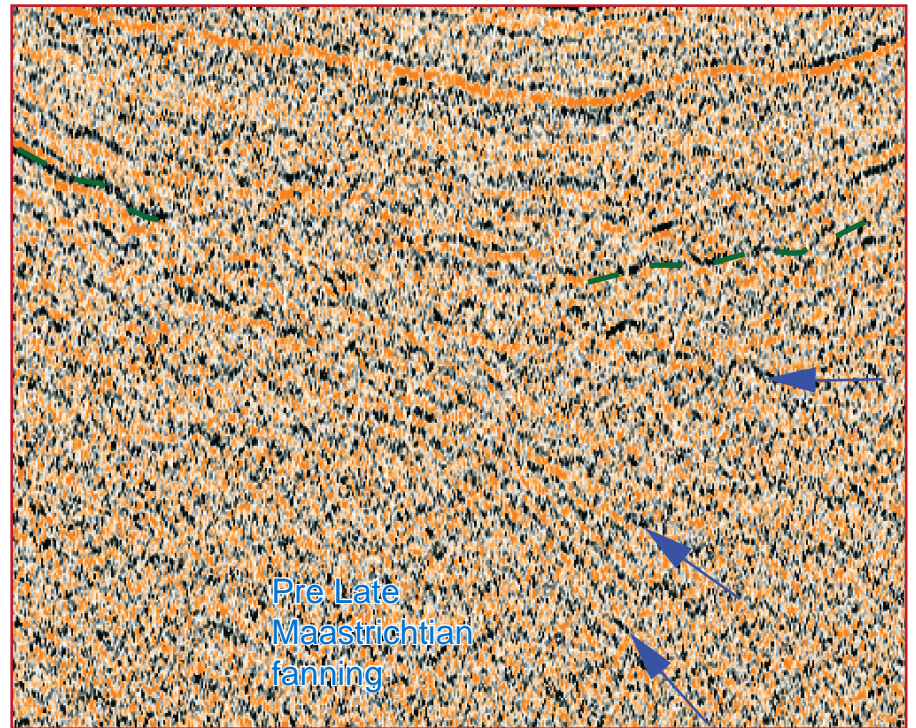


Figure C

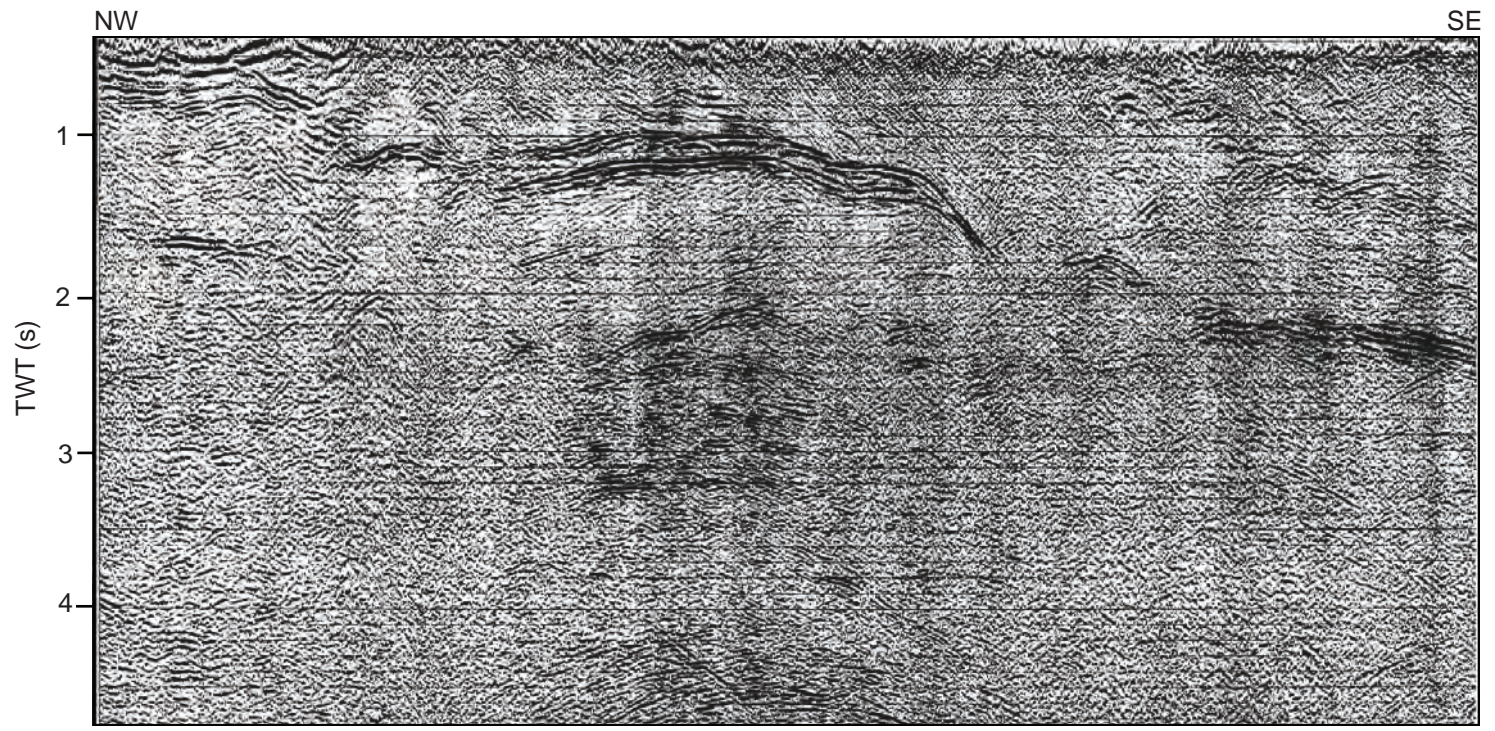


★ Boundary of pre-Late Maastrichtian grabens on seismic lines

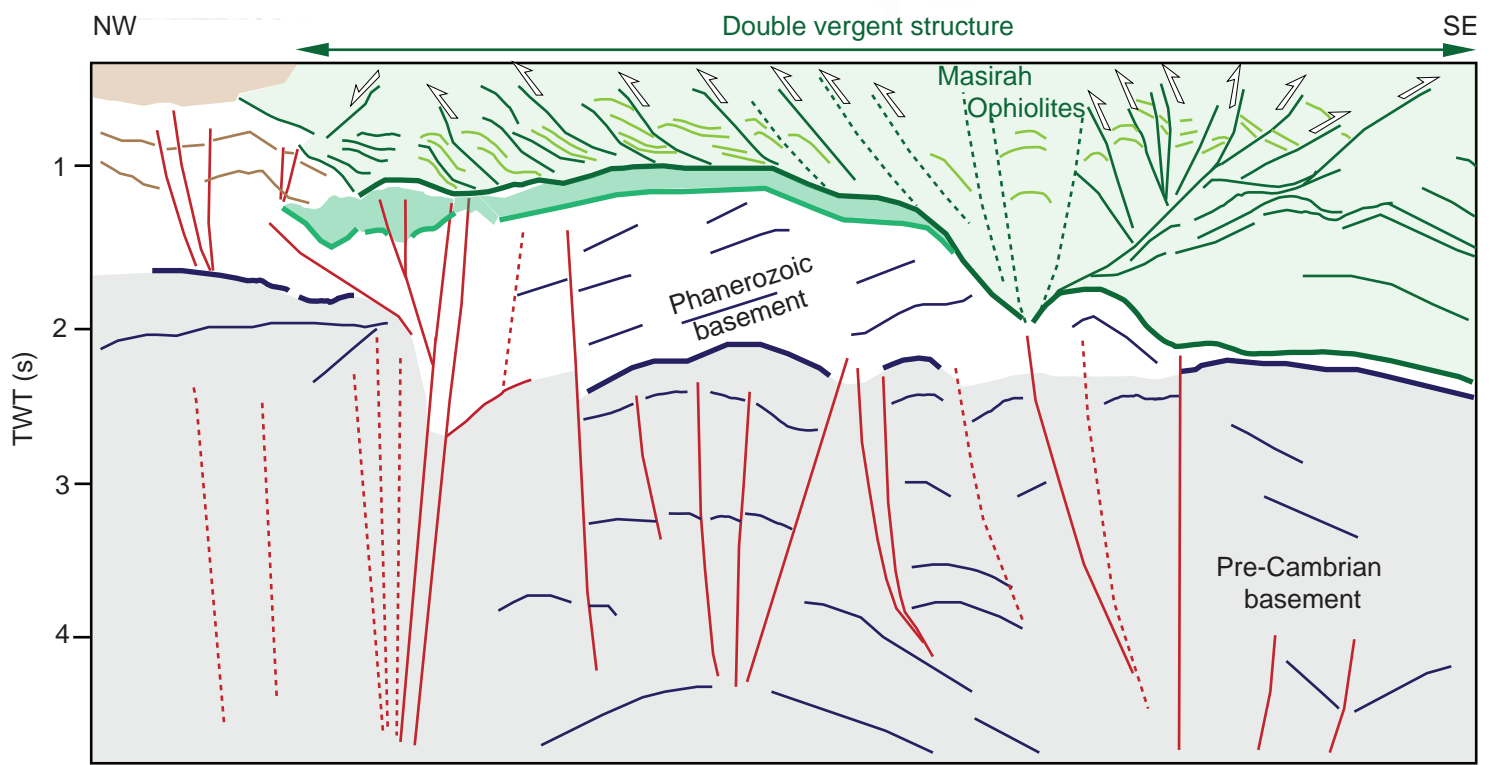
ZOOM Line C

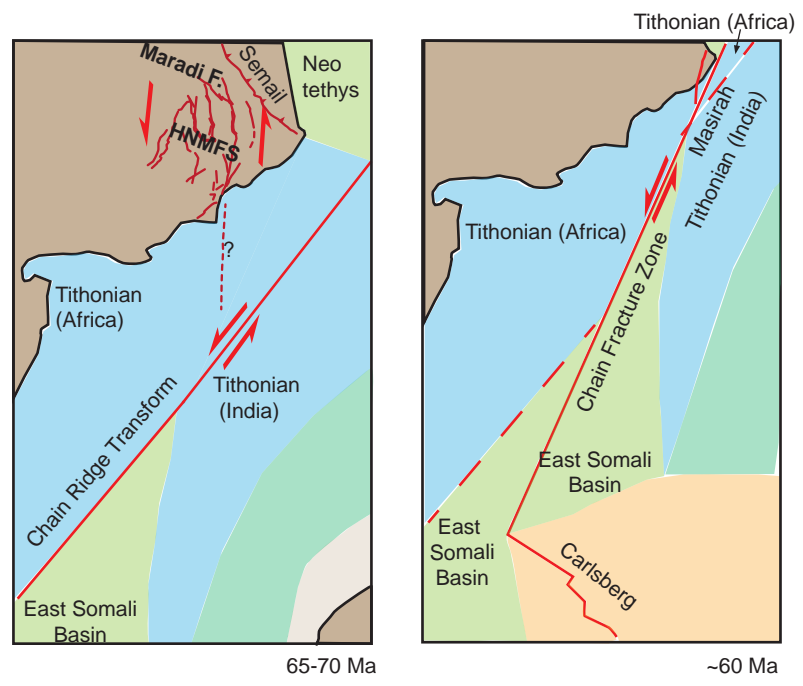


Figure

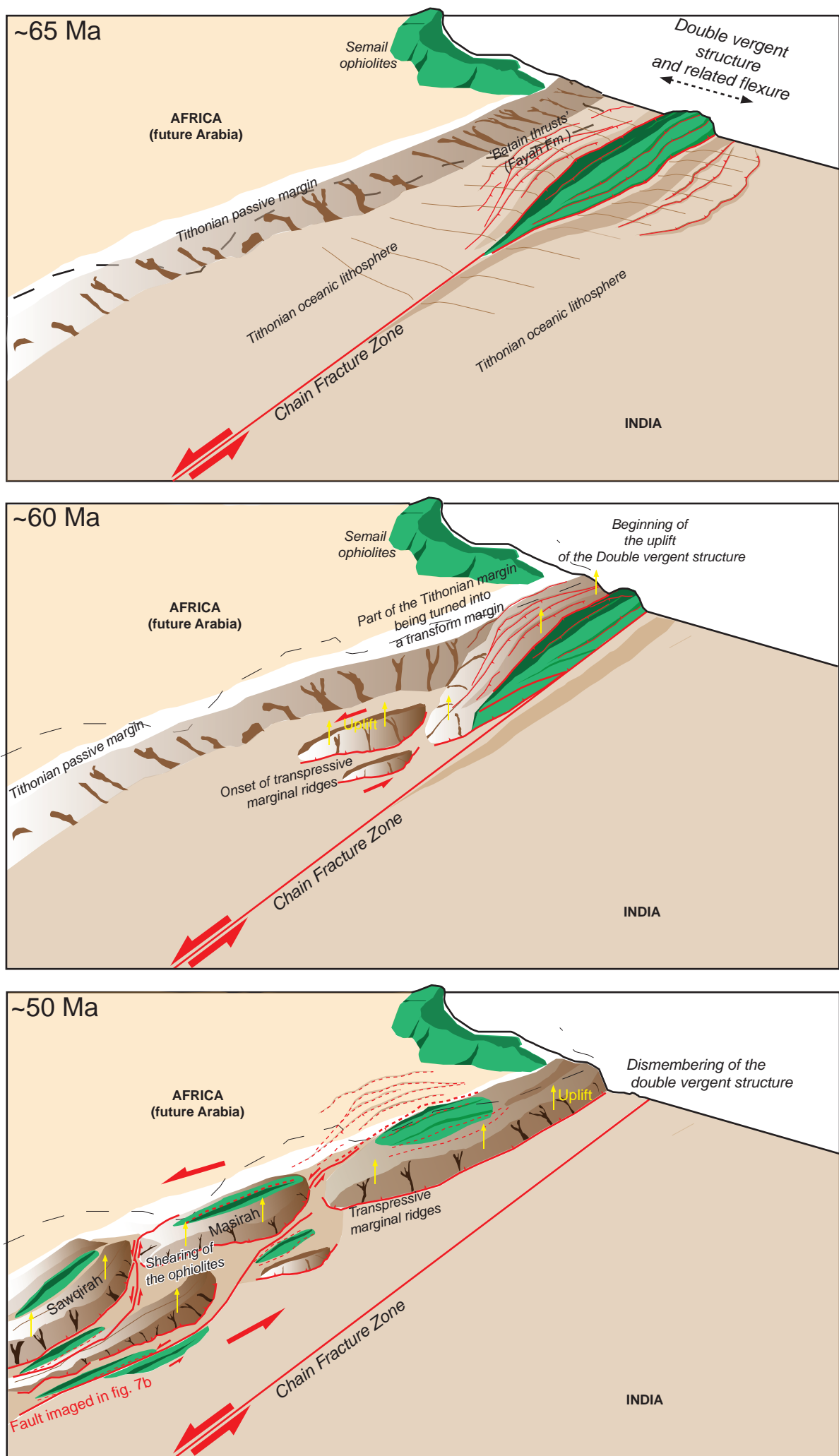


Profile from Beauchamp et al., 1995

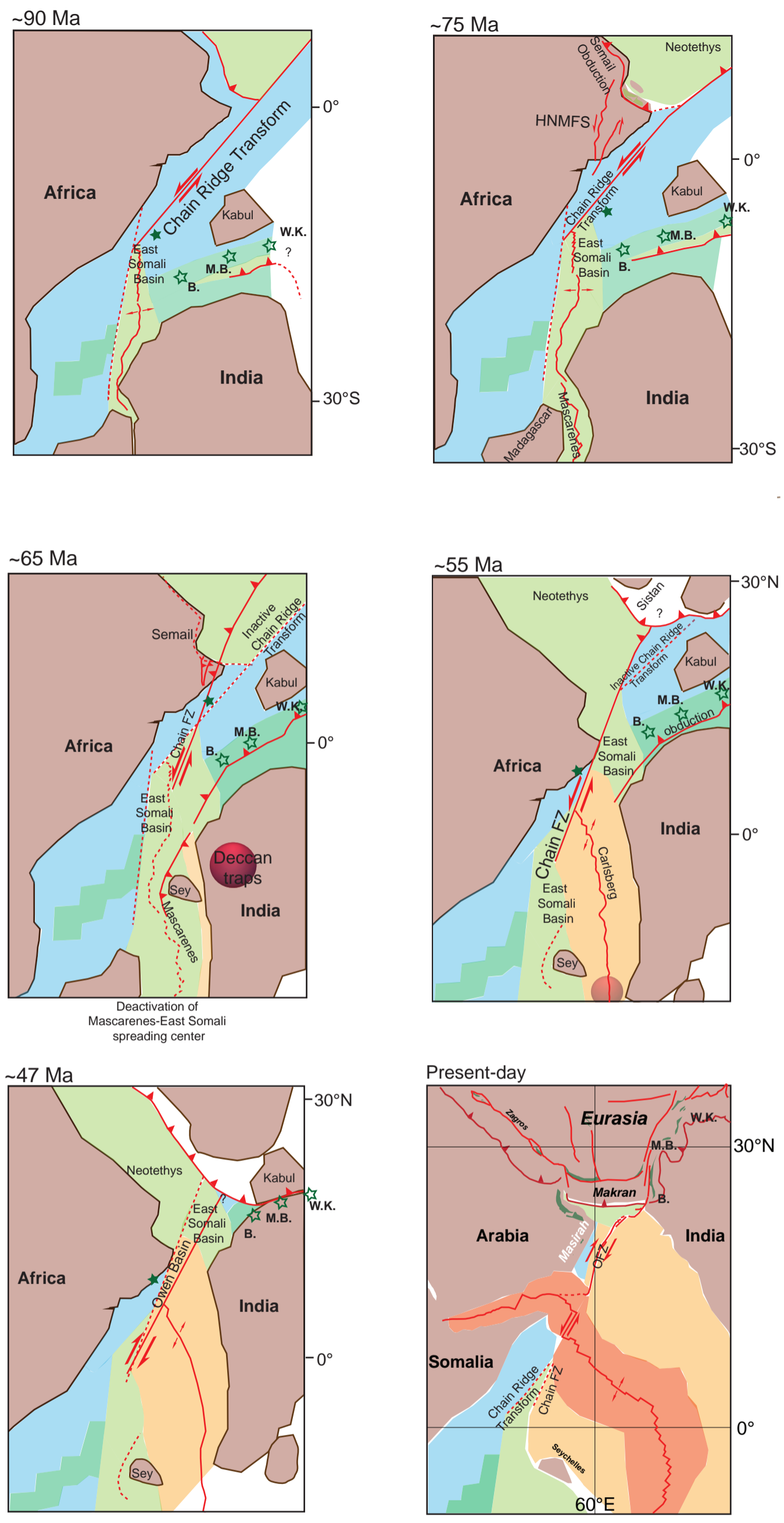




Figure



Figure



Seafloor age

- Late Jurassic - Early Cretaceous
- Early-Middle Cretaceous
- Late Cretaceous
- Paleogene
- Neogene

- Masirah oceanic lithosphere
  - B. : Bela
  - M.B.: Muslim Bagh
  - W.K.: Waziristan Khost
- } oceanic lithosphere
- Strike-slip boundary
  - Divergent boundary
  - Convergent boundary